Long-term patterns of an interconnected core marine microbiota

Anders K. Krabberød[1*], Ina M. Deutschmann[2], Marit F. M. Bjorbækmo[1], Vanessa Balagué[2], Caterina R. Giner[2], Isabel Ferrera[2,3], Esther Garcés[2], Ramon Massana[2], Josep M. Gasol[2, 4], Ramiro Logares[2,1*]

[1] University of Oslo, Department of Biosciences, Section for Genetics and Evolutionary Biology (Evogene), Blindernv. 31, N-0316 Oslo, Norway

[2] Institute of Marine Sciences (ICM), CSIC, Passeig Marítim de la Barceloneta, Barcelona, Spain

[3] Centro Oceanográfico de Málaga, Instituto Español de Oceanografía, 29640 Fuengirola, Málaga, Spain

[4] Centre for Marine Ecosystems Research, School of Sciences, Edith Cowan University, Joondalup, WA, Australia

Corresponding authors:

*Anders K. Krabberød, University of Oslo, Department of Biosciences, Section for Genetics and Evolutionary Biology (Evogene), Blindernv. 31, N-0316 Oslo, Norway
Email: a.k.krabberod@ibv.uio.no

*Ramiro Logares, Institute of Marine Sciences (ICM), CSIC, Passeig Marítim de la Barceloneta, Barcelona, Spain
Email: ramiro.logares@icm.csic.es

Running title: Patterns in a core marine microbiota

Manuscript for: Microbiome

ABSTRACT

Background

Ocean microbes constitute ~70% of the marine biomass, are responsible for ~50% of the Earth's primary production, and are crucial for global biogeochemical cycles. Marine microbiotas include core taxa that are usually key for ecosystem function. Despite their importance, core marine microbes are relatively unknown, which reflects the lack of consensus on how to identify them. So far, most core microbiotas have been defined based on species occurrence and abundance. Yet, species interactions are also important to identify core microbes, as communities include interacting species. Here, we investigate interconnected bacteria and small protists of the core pelagic microbiota populating a long-term marine-coastal observatory in the Mediterranean Sea over a decade.

Results

Core microbes were defined as those present in >30% of the monthly samples over 10 years, with the strongest associations. The core microbiota included 259 Operational Taxonomic Units (OTUs) including 182 bacteria, 77 protists, and 1,411 strong and mostly positive (~95%) associations. Core bacteria tended to be associated with other bacteria, while core protists tended to be associated with bacteria. The richness and abundance of core OTUs varied annually, decreasing in stratified warmers waters and increasing in colder mixed waters. Most core OTUs had a preference for one season, mostly winter, which featured subnetworks with the highest connectivity. Groups of highly associated taxa tended to include protists and bacteria with predominance in the same season, particularly winter. A group of 13 highly-connected hub-OTUs, with potentially important ecological roles dominated in winter and spring. Similarly, 18 connector OTUs with a low degree but high centrality were mostly associated with summer or autumn and may represent transitions between seasonal communities.

Conclusions

We found a relatively small and dynamic interconnected core microbiota in a model temperate marine-coastal site, with potential interactions being more deterministic in winter than in other seasons. These core microbes would be essential for the functioning of this ecosystem over the year. Other non-core taxa may also carry out important functions but would be redundant and non-essential. Our work contributes toth e understanding of the dynamics and potential interactions of core microbes possibly sustaining ocean ecosystem function.

Keywords: bacteria, protists, ocean, time-series, seasonality, networks, associations

BACKGROUND

Ecosystems are composed of interacting units embedded in and influenced by their physicochemical environment. Ecosystem function can be broadly defined as the biological, geochemical, and physical processes that occur within it. These processes will likely change or halt if specific organisms or gene-functions are removed, driving the ecosystem towards a new state or its collapse. It is hypothesized that ecological redundancy guarantees continuous ecosystem function, as multiple species could carry out the same or similar function [1]. And while the amount of functional redundancy in microbial ecosystems is a matter of debate [2, 3] it has also been observed that microbiotas in comparable habitats tend to share "core" species that are hypothesized to be fundamental for ecosystem function [4]. These core organisms and the functions they carry out might not be easily replaced.

Identifying the core microbiota is not straightforward as there are different ways of defining a core depending on the habitats and the questions being addressed [4]. One often-used approach is to identify species that tend to be recurrently present across spatiotemporal scales. This definition might not be sufficient, however, since communities are made up of interacting species [5]. A more appropriate definition of a core, therefore, needs to incorporate ecological interactions fundamental for the community in the location under study [4, 5]. This is particularly important in studies using DNA to investigate microbial communities, as a fraction of the detected taxa could be dormant, dead, or transient [6-8]. In the interaction-based definition taxa that do not appear to be interacting are excluded from the core [4].

Core microbiotas based on common presence have been widely studied in terrestrial animals, in particular humans [9] or cattle [10], as well in marine animals, in particular corals [11, 12] and sponges [13, 14]. Core microbiotas in non-host-associated

systems, such as soils or the ocean, have been investigated to a lesser extent. In soils, for example, a global analysis identified a core group of 241 ubiquitous and dominant bacterial taxa with more or less invariant abundances and unclear habitat preferences [15]. In the tropical and subtropical global-ocean, a total of 68 bacteria and 57 picoeukaryotic operational taxonomic units (OTUs) have been identified that could be part of the core surface microbiota, as they were present in >80% of the globally-distributed samples [16].

Analyses of ocean time-series have also pointed to the existence of core microbiotas. For example, Gilbert et al. [17] investigated the microbiota of the English Channel for 6 years and found 12 abundant OTUs that were detected throughout the entire dataset (72 time-points), totaling ~35% of the sequence abundance. Potentially core bacterial OTUs were detected in the SPOT time-series (southern California), in a study covering 10 years of monthly samples in the euphotic zone [18]. These potentially-core bacterial OTUs were present in >75% of the months, represented ~7% (25-28 OTUs depending on depth) of the total richness, and had a high (>10%) relative abundance [18].

These studies have provided substantial insights on core marine microbiotas, although they typically define them in terms of species occurrence or abundance over spatiotemporal scales, rather than on potential interactions. As in other ecosystems, microbial interactions are essential for the functioning of the ocean ecosystem, where they guarantee the transfer of carbon and energy to upper trophic levels, as well as the recycling of carbon and nutrients [19]. Despite their importance, most microbial interactions in the ocean remain unknown [20]. A recent literature survey spanning the last 150 years indicated that we have documented a minor fraction of protist interactions in the ocean [21] and most likely, the same is true if not worse for bacteria.

132 During the last decade, association networks have been used to bridge this
133 knowledge gap. Association networks are based on correlations between species'
134 abundances and they may reflect microbial interactions [22]. Contemporaneous
135 positive correlations may point to interactions such as symbiosis, or similar niche
136 preferences, while negative correlations may suggest predation, competition, or
137 opposite niche preferences [23]. So far, network analyses have produced hypotheses on
138 microbial interactions at the level of individual species across diverse ecosystems [22,
139 24, 25], a few of which have been experimentally validated [26]. In addition, networks
140 can help detect species that have relatively more associations to other species ("hubs"),
141 or species that connect different subgroups within a network, and which therefore may
142 have important roles in the ecosystem. Groups of highly associated species in the
143 network ("modules") may represent niches [27, 28], and the amount of these modules
144 may increase with increasing environmental selection [22]. Networks can also produce
145 ecological insight at the community level, since their architecture can reflect
146 community processes, such as selection [27].

147 Network analyses have been particularly useful for the investigation of
148 microbial interactions in the ocean [25, 29]. A surface global-ocean network analysis
149 of prokaryotes and single-celled eukaryotes indicated that ~72% of the associations
150 between microbes were positive and that most associations were between single-celled
151 eukaryotes belonging to different organismal size-fractions [26]. Other studies using
152 networks have indicated a limited number of associations between marine microbes and
153 abiotic environmental variables [17, 18, 23, 26, 30-32], suggesting that microbial
154 interactions have an important role in driving community turnover [32]. Despite the
155 important insights these studies have provided, most of them share the limitation that

156 they do not disentangle whether microbial associations may represent ecological
157 interactions or environmental preferences [22].

158 Even though association networks based on long-term species dynamics may
159 allow a more accurate delineation of core marine microbiotas, few studies have
160 identified them in this manner. Consequently, we have a limited understanding of the
161 interconnected set of organisms that may be key for ocean ecosystem function. Here
162 we identify and investigate the core microbiota occurring in the marine-coastal Blanes
163 Bay Microbial Observatory (Northwestern Mediterranean Sea) over 10 years. We
164 delineated the core microbiota stringently, using potential interactions based on species
165 abundances. We also made an effort to disentangle environmental effects in association
166 networks by identifying and removing species associations that are a consequence of
167 shared environmental preference and not interactions between the species [33]. We
168 analyzed bacteria and protists from the pico- (0.2-3 µm) and nanoplankton (3-20 µm)
169 organismal size fractions, which show a strong seasonality in this location [34-36].
170 Taxa relative abundances were estimated by sequencing the 16S and 18S rRNA-gene
171 and delineating OTUs as Amplicon Sequence Variants (ASVs). Specifically, we ask:
172 What taxa constitute the interconnected core microbiota and what are the main patterns
173 of this assemblage over 10 years? Does the core microbiota feature seasonal sub-groups
174 of highly associated species? What degree of association do bacteria and microbial
175 eukaryotes have and do they show comparable connectivity? Can we identify core
176 OTUs with central positions in the network that could have important ecological roles?
177

178 **RESULTS**

179 *Composition and dynamics of the resident microbiota*

180 Based on the data set containing 2,926 OTUs, (1,561 bacteria and 1,365 microbial
181 eukaryotes) we first defined the resident OTUs as the bacteria and microbial eukaryotes
182 present in >30% of the samples, which equals 36 out of 120 months (not necessarily
183 consecutive). This threshold was selected as it includes seasonal OTUs that would be
184 present recurrently in at least one season. The residents consisted of 709 OTUs: 354
185 Bacteria (~54% relative read abundance) and 355 Eukaryotic OTUs (~46% relative
186 read abundance) [**Table 1,** see methods for calculation of relative read abundance]. The
187 most abundant resident bacteria OTUs belonged to Oxyphotobacteria (mostly
188 *Synechococcus*; ~15% of total relative read abundance), Alphaproteobacteria (mostly
189 SAR11 Clade Ia [~9%, and clade II [~4%]), and Gammaproteobacteria (mainly SAR86;
190 ~2%). The most abundant resident protist OTUs belonged to Dinophyceae
191 (predominantly an unclassified dinoflagellate lineage [~7%], Syndiniales Group I
192 Clade 1 [~7%] and *Gyrodinium* [~4%]), Chlorophyta (mostly *Micromonas* [~3%] and
193 *Bathycoccus* [~2%]), Ochrophyta (predominantly Mediophyceae [~2%] and
194 *Chaetoceros* [~1%]) and Cryptophyceae (mainly a Cryptomonadales lineage [~2%])
195 [**Figure 3, Table S1**].
196
197
198 **Table 1.** Description of the datasets

	OTUs	OTUs (%)	Sequence abundance (%)*
All OTUs[1]	2,926	100	*100*
Bacteria	1,561	53.3	*50.7*
Protists	1,365	46.7	*49.3*
Resident microbiota[2]	709	100	100 (*85*)
Bacteria	354	49.9	53.6
Protists	355	50.1	46.4
Core microbiota[3]	**259**	**100**	**64.5 (*54*)**
Bacteria	182	70.3	46.3
Protists	77	29.7	18.2
Picoplankton	109	42.1	32.4
Nanoplankton	150	57.9	32.1
Protists			
Heterotroph	5	1.9	0.3
Photoautotroph	37	14.3	11.8

Parasite	21	8.1	3.5
Mixotroph	3	1.2	0.7
Symbiont	1	0.4	0.1
Unknown	11	4.3	2.0
Bacteria			
Photoautotroph (cyanobacteria)	19	7.3	19.3
Non-photoautotroph[4]	163	62.5	26.8
Seasonal preference core OTUs			
Winter	156	60.2	21.8
Spring	24	9.3	16.4
Summer	44	17.0	8.2
Autumn	30	11.6	13.7
No seasonality	5	1.9	4.5
Seasonal subnetworks			
Winter	156	60.2	21.8
Spring	19	7.3	13.7
Summer	41	15.8	6.6
Autumn	26	10.0	12.9

[1] Number of OTUs in the full dataset that were left after quality control and rarefaction, which were present in at least 10% of the samples (i.e. 12 months, not necessarily consecutive).
[2] OTUs present in at least 30% of the samples (i.e. 36 months, not necessarily consecutive) [=Resident microbiota].
[3] OTUs included in the core network (core microbiota) with significant correlations (p&q <0.001), local similarity scores >|0.7| and Spearman correlations >|0.7|, being present in at least 30% of the samples.
[4] Includes non-photoautotrophic lifestyles (i.e., chemoautotrophs, photoheterotrophs, chemoheterotrophs, etc.).
* In *Italics* the abundances relative to all OTUs are indicated. All other values in normal text indicate abundances relative to OTUs in the resident microbiota.

The resident microbiota, including both protists and bacteria, showed seasonal variation over 10 years, with communities from the same season but different years tending to group (**Figure 1C and D**). The structure of the resident microbiota correlated to specific environmental variables during winter (nutrients, Total photosynthetic nanoflagellates [PNF; 2-5µm size], and small PNF [2µm]), spring (Total Chlorophyll a [Chla]), summer (daylength, temperature, Secchi disk depth and, the cell abundances of *Synechococcus,* Heterotrophic prokaryotes [HP] and Heterotrophic nanoflagellates [HNF, 2-5µm]) and autumn (salinity) [**Figure 1C**]. The environmental variables most relevant for explaining the variance of the resident microbiota were determined by stepwise model selection and distance-based redundancy analyses (dbRDA) [**Figure 1D**], leading to a dbRDA constrained and unconstrained variation of 41% and 59% respectively (**Figure 1D**). The selected variables were predominantly aligned with the axis summer (daylength, temperature, and the cell abundance of *Synechococcus* and HP) - winter (SiO_2, small PNF [**Figure 1D**]. This dbRDA axis had the highest eigenvalue, explaining ~55% of the constrained variation (**Figure 1D**). Even though

223 the measured environmental variables did not explain the majority of the variation of
224 the resident microbiota, they could account for a substantial fraction. This was further
225 supported by Adonis analyses, which indicated that the measured environmental
226 variables could explain ~45% of the resident microbiota variance, with temperature and
227 daylength having a predominant role by accounting for 30% of this variance (15%
228 each).

229 We then investigated whether temperature and daylength could determine the
230 main niches. We found that ~70% and ~68% of the OTUs in the resident microbiota
231 had niche preferences associated with temperature or daylength respectively (**Figure**
232 **1E-F**; Note that several OTUs preferring Spring or Autumn are not expected to be
233 detected with this approach, as their preferred temperature or daylength may not differ
234 significantly from the randomized mean). In total, 371 OTUs from the resident
235 microbiota had both a temperature and a daylength niche preference that departed
236 significantly from the randomization mean (**Figure 1E-F**). These 371 OTUs
237 represented ~52% of all OTUs in the resident microbiota, corresponding to ~90% of
238 the sequence abundance. In particular, 248 OTUs had a weighted mean for both
239 temperature and daylength below the randomization mean (corresponding to
240 winter/autumn), while 116 OTUs had a weighted mean above the randomization mean
241 for both variables (corresponding to summer/spring). Interestingly, 7 OTUs displayed
242 a weighted mean above and below the randomized mean for temperature and daylength
243 respectively (corresponding to autumn or spring).

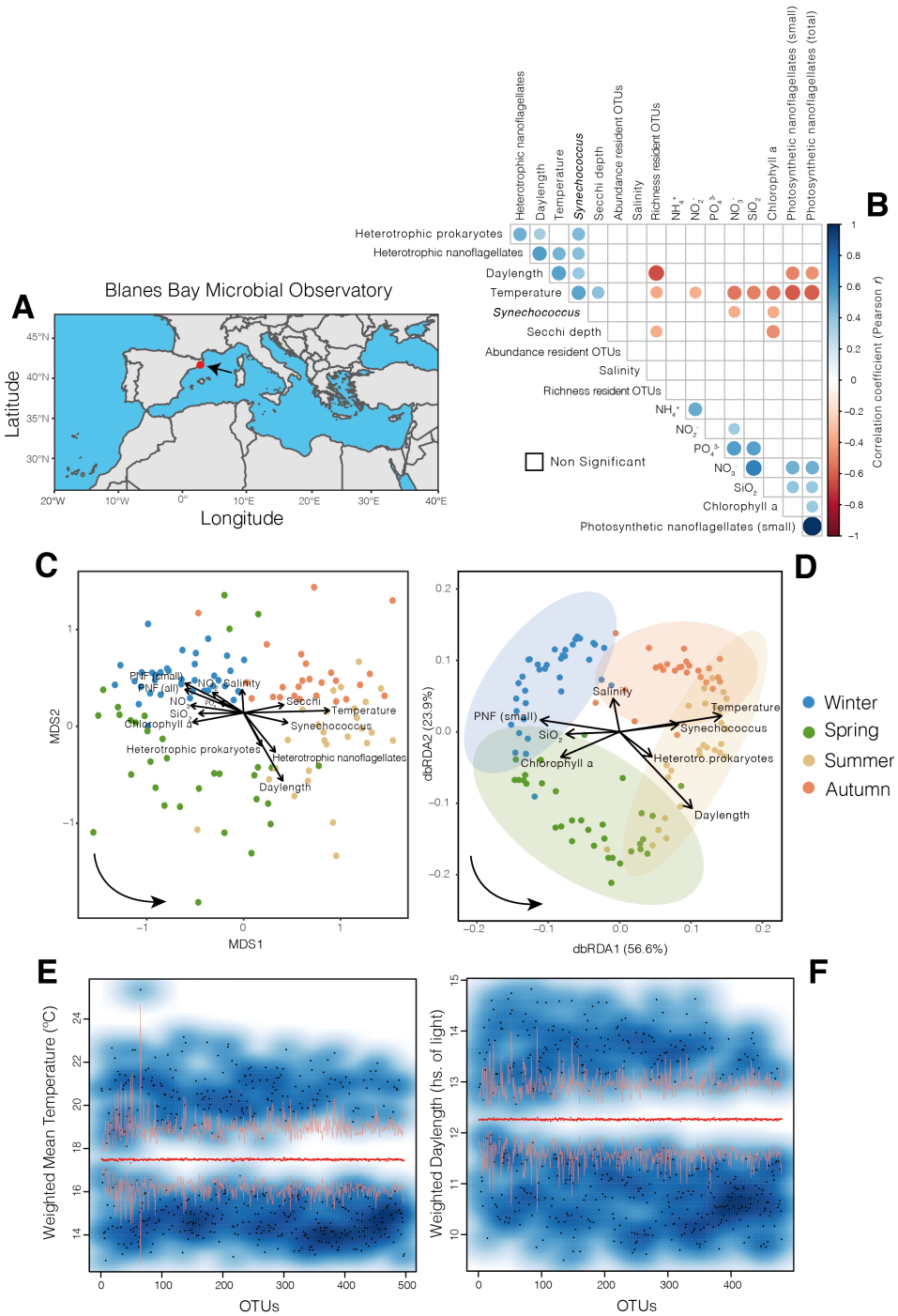

Figure 1. The Blanes Bay Microbial Observatory and the variation of its resident microbiota and measured environmental variables over ten years. A) Location of the Blanes Bay Microbial Observatory. **B)** All possible correlations between the measured environmental variables including the richness and abundance of resident OTUs (NB: only 709 resident OTUs are considered, see **Table1**). Only significant Pearson correlation coefficients are shown (p<0.01). The p-values were corrected for multiple inference (Holm's method). **C)** Unconstrained

251 ordination (NMDS based on Bray Curtis dissimilarities) of communities including resident OTUs
252 only, to which environmental variables were fitted. Only variables with a significant fit are shown
253 (P<0.05). Arrows indicate the direction of the gradient and their length represents the strength
254 of the correlation between resident OTUs and a particular environmental variable. The color of
255 the samples (circles) indicates the season to which they belong. The bottom-left arrow indicates
256 the direction of the seasonal change. PNF = photosynthetic nanoflagellates. **D)** Constrained
257 ordination (Distance-based redundancy analyses, dbRDA, using Bray Curtis dissimilarities)
258 including only the most relevant variables after stepwise model selection using permutation tests.
259 Each axis (i.e., dbRDA1 and dbRDA2) indicates the amount of variance it explains according to
260 the associated eigenvalues. The color of the samples (circles) indicates the season to which they
261 belong. Arrows indicate the direction of the gradient and their length represents the strength of
262 the correlation between resident OTUs and a particular environmental variable. The bottom-left
263 arrow indicates the direction of the seasonal change. E-F) Resident OTUs displaying different
264 niche preferences (blueish areas) in terms of the two most important abiotic variables:
265 Temperature E) and Daylength F). The red dots indicate the randomization mean, and the orange
266 curves represent the confidence limits. Black dots indicate individual OTUs for which temperature
267 or daylength preferences are significantly (p<0.05) higher or lower than a random distribution
268 over 10 years. At least two assemblages with different niches become evident: one preferring
269 higher temperature and longer days (summer/spring), and another one preferring lower
270 temperature and shorter days (winter/autumn). Note that several OTUs associated to Spring or
271 Autumn are not expected to be detected with this approach, as their preferred temperature or
272 daylength may not differ significantly from the randomized mean.
273
274 *Core network*

275 To determine the core microbiota that incorporates possible interactions, we
276 constructed an association network based on the resident OTUs and removed all OTUs
277 that were not involved in strong and significant associations with any other OTUs.
278 Specifically, we kept only the associations (edges in the network) with Local similarity
279 score |LS| > 0.7, a false discovery rate adjusted p-value < 0.001 and Spearman |r| > 0.7.
280 In addition, we removed all associations that seemed to be caused by environmental
281 preferences of OTUs (see Methods). The core network consisted of 1,411 significant
282 and strong correlations (**Figure 2A**) and was substantially smaller than the network
283 based on the resident OTUs without stringent cut-offs (**Supp. Figure 1A**, removed
284 edges in **Supp. Figure 1B**). The core network includes only the strongest microbial
285 associations that are inferred during a decade and, according to our definition,
286 determines the core microbiota. The associations in the core microbiota may represent
287 proxies for species interactions since steps have been taken to remove associations that
288 are driven by environmental factors.

289 In the core network, most associations were positive (~95%), pointing to the
290 dominance of co-existence or symbiotic associations (**Table 2, Figure 2A**). The core
291 network had "small world" properties [37], with a small average path length (i.e.
292 number of nodes between any pair of nodes through the shortest path) and a relatively
293 high clustering coefficient, showing that nodes tend to be connected to other nodes,
294 forming tightly knit groups, more than what it would be expected by chance (**Table 3**).
295 Since node degree was not correlated with OTU abundance (**Supp. Figure 2**), the
296 associations between OTUs are not caused by a high sequence abundance alone, as the
297 most abundant OTUs did not tend to be the most connected.

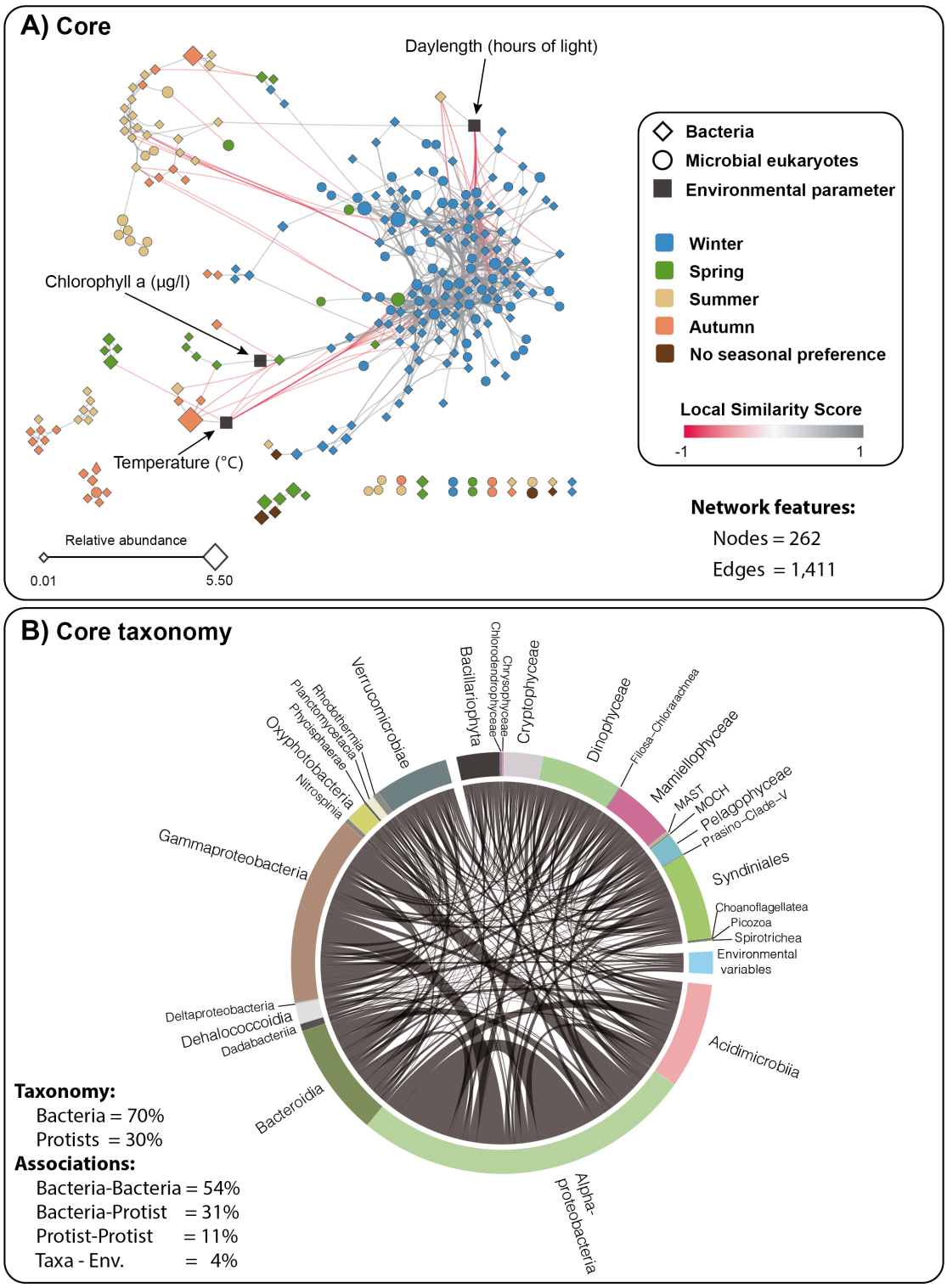

Figure 2. Core microbiota resulting from 10 years of monthly pico- and nanoplankton relative abundances. A) Core network including bacteria and microbial eukaryotic OTUs that occur ≥ 30% of the time during the studied decade (i.e. resident microbiota), with highly significant and strong associations (P<0.001 and Q<0.001, absolute local similarity score |LS| >

304 0.7, Spearman correlation |ρ|>0.7), where detected environmentally-driven edges were
305 removed. The color of the edges (links) indicates whether the association is positive (grey) or
306 negative (red). The shape of nodes indicates bacteria (rhomboid) or microbial eukaryotes (circle),
307 and the color of nodes represents species seasonal preferences, determined using the indicator
308 value (*indval*, p<0.05). Node size indicates OTU relative abundance. B) Core network as a Circos
309 plot, indicating the high-rank taxonomy of the core OTUs. Since 95% of the associations are
310 positive (see Table 2), we do not indicate whether an edge is positive or negative.
311

312 The core network displayed a winter cluster, while no clear clusters could be
313 defined for the other seasons (**Figure 2A**). Of the 15 environmental variables analyzed,
314 only 3 were found to be significantly correlated with core OTUs: *daylength*, showing
315 strong correlations with 33 OTUs, *temperature*, correlated with 14 OTUs, and
316 *Chlorophyll a*, correlated with 1 OTU (**Figure 2A**). Therefore, the analysis of the core
317 network also points to the importance of temperature and daylength in the decade-long
318 seasonal dynamics of the studied microbial ecosystem. It is also coherent with the
319 Adonis and ordination analyses (**Figure 1C-B**). However, the associations between
320 these environmental parameters with taxa represented only 4% of all the associations
321 (**Figure 2B**).

322 **Table 2.** Core associations. See **Figure 2**.
323

	Association # (edges)	Co-occurrences (positive)	Co-exclusions (negative)
All	1,411	1,341 (95.0%)	70 (5.0%)
Within Picoplankton	378	353 (93.3%)	25 (6.6%)
Within Nanoplankton	791	748 (94.6%)	43 (5.4%)
Picoplankton-Nanoplankton	242	240 (99.2%)	2 (0.8%)

324

325 Of the 709 OTUs from the resident microbiota (**Figure 3**), only 259 OTUs
326 (35%) were left in the core network (182 bacteria (~70%) and 77 microbial eukaryotic
327 OTUs (~30%); **Table 1, Figure 2**). The monthly taxonomic composition of the resident
328 microbiota differed from that of the core (**Figure 3**). The core OTUs accounted for
329 ~64% of the relative read abundance of the resident microbiota (**Table 1**). The core

OTUs had annual variation in terms of richness and abundance over the 10 years for both the pico- and nanoplankton, with microbial eukaryotes decreasing markedly in OTU richness and relative read abundance in the warmer seasons, and increasing during colder periods (**Figure 3**).

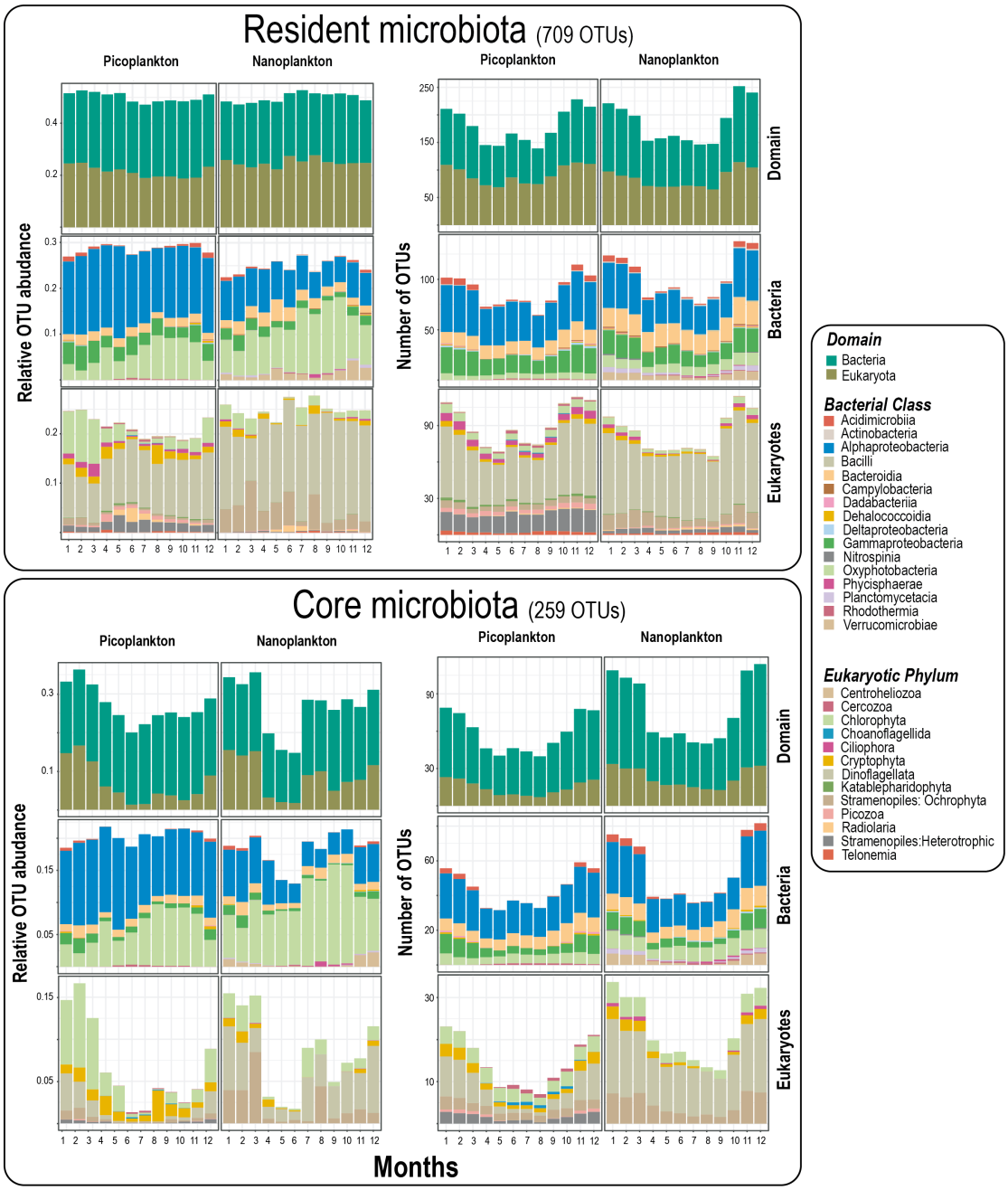

Figure 3. The monthly variation in the resident and core microbiotas over 10 years. *Upper panels:* The resident microbiota is defined as those eukaryotes and bacteria that occur in at least

338 30% of the samples over 10 years. The relative OTU abundance (left panel) and number of OTUs
339 (right panel) for different domains and taxonomic levels in the resident microbiota are shown.
340 Note that the relative abundance of Bacteria vs. Eukaryotes does not necessarily reflect
341 organismal abundances on the sampling site, but the amplicon relative abundance after PCR.
342 Relative abundances were calculated for each year and aggregated over the corresponding
343 months along the 10 years for the resident microbiota, then split into size fractions (NB: relative
344 abundance for both domains and size fraction sums up to 1 for each month across ten years).
345 *Lower panels:* Core microbiota over 10 years. The relative abundances of core OTUs reflect the
346 remaining proportions after removing all the OTUs that were not strongly associated when
347 building networks. Relative OTU abundance (left panel) and number of OTUs (right panel) for
348 different domains and taxonomic levels among the core OTUs.
349
350 The most abundant bacteria (**Figure 3**; **Supplementary Table S2**) among the
351 core OTUs were Oxyphotobacteria (mostly *Synechococcus*), total abundance ~14% of
352 the resident microbiota, followed by Alphaproteobacteria, with SAR11 clades Ia and II
353 representing ~9% and ~2% respectively. The most abundant microbial eukaryotic
354 groups were *Micromonas*, *Bathycoccus*, Dinophyceae, and Cryptomonadales (each
355 ~2%) [**Figure 3**; **Supplementary Table S3**]. In terms of diversity and abundance,
356 bacterial non-phototrophs (including chemoautotrophs, photoheterotrophs,
357 chemoheterotrophs) were the most prevalent in the core microbiota, representing ~62%
358 of the OTUs and a quarter of the total relative read abundance (**Table 1**). In turn,
359 protistan heterotrophs represented a minor fraction of the diversity and relative
360 abundance **(Table 1)**. Bacteria photoautotrophs were relatively more abundant than
361 their protistan counterparts but less diverse (**Table 1**). Protistan parasites represented

362 ~8% of the OTUs and ~3% of the abundance, while the remaining protistan lifestyles
363 had a minor relevance in the core microbiota (**Table 1**).
364
365 *Intra- and cross-domain core associations*
366 Bacteria tended to be associated with other bacteria (**Table 3 & 4**; **Figure 2B**), with
367 Bacteria-Bacteria associations making up ~54% of all associations, while Protist-Protist
368 associations accounted for 11% (**Table 4**). The connectivity of the bacterial
369 subnetworks was higher (mean degree ~10) than the protist counterparts (mean degree
370 ~6), regardless of whether these networks included exclusively bacteria, protists, or
371 both (**Table 3**).
372 In particular, there was a substantial number of associations between Alpha-
373 and Gammaproteobacteria, between Alphaproteobacteria and Acidiimicrobia as well as
374 among Alphaproteobacteria OTUs (**Figure 2B**). Eukaryotic OTUs did not show a
375 similar trend with associations between OTUs of the same taxonomic ranks (**Figure**
376 **2B**). In terms of cross-domain associations, Alphaproteobacteria OTUs had several
377 associations with most major protistan groups (i.e. dinoflagellates, diatoms,
378 cryptophytes, Mamiellophyceae, and Syndiniales) [**Figure 2B**].
379
380 *Core associations within the pico- and within the nanoplankton*
381 While the pico- and nano-size fractions indicate different lifestyles in bacteria (free-
382 living or particle-attached), they indicate different cell sizes in protists, and this could
383 be reflected in association networks. Nanoplankton sub-networks were larger and more
384 connected than picoplankton counterparts (**Figure 4**, **Table 3**). This pattern was
385 observed in both sub-networks considering associations from the same or both size
386 fractions (**Table 3**). Nanoplankton sub-networks had a higher average degree (~10)

387 than picoplankton sub-networks (~7; Wilcoxon $p<0.05$), while not differing much in
388 other network statistics (**Table 3**). Most associations in the pico- and nanoplankton
389 were positive (>93%), while the associations between OTUs from different size
390 fractions represented only ~17% of the total, being ~99% positive (**Table 2**).

391 In the pico- or nanoplankton sub-networks that include OTUs from the same
392 size fraction, the number of bacterial core OTUs was higher than the protistan
393 counterparts (103 bacterial vs. 47 protistan OTUs in the nanoplankton, and 79 bacterial
394 vs. 30 protistan OTUs in the picoplankton) (**Figure 4**, **Table 3**). Still, core OTUs in
395 both the pico- and nanoplankton had comparable sequence abundances: ~27% of the
396 resident microbiota in each size fraction. Within the picoplankton, 64% of the
397 associations were between bacteria, 8% between eukaryotes, and 25% between
398 eukaryotes and bacteria (**Table 4**). In turn, in the nanoplankton, 50% of the edges were
399 between bacteria, 14% between eukaryotes, and 31% between eukaryotes and bacteria
400 (**Table 4**). Overall, the BBMO pico- and nanoplankton sub-networks differed in size,
401 connectivity, and taxonomic composition, while they were similar in terms of positive
402 connections and relative sequence abundance.

403

404 **Table 3.** Core network and sub-networks statistics.

Network	Nodes (#OTUs)	Edges	Di.	De.	Average degree	Average path length	Average clustering coefficient	Largest clique (#)	Mod.
Core network	262 (259)	1,411	11	0.04	10.7	3.45	0.52	13 (4)	0.19
Random core network	262	1,411	5	0.04	10.7	2.60	0.03	3(199)	0.13
Picoplankton all [1]	161 (160)*	620*	10	0.05	7.7	3.13	0.55	10(1)	0.22
Picoplankton only [2]	110 (109)	378	9	0.06	6.9	3.15	0.51	9(4)	0.29
Nanoplankton all [3]	197 (194)*	1,033*	10	0.05	10.5	3.18	0.57	13(4)	0.15
Nanoplankton only[4]	153 (150)	791	10	0.07	10.3	3.21	0.56	13(4)	0.17
Bacteria all [5]	233 (230)**	1,236**	10	0.04	10.6	3.34	0.52	11(3)	0.19
Bacteria only [6]	185 (182)	803	10	0.05	8.7	3.50	0.51	10(1)	0.31
Protists all [7]	147 (145)**	608**	5	0.06	8.3	2.40	0.48	8(2)	0.10
Protist only [8]	80 (77)	175	5	0.05	4.4	2.54	0.54	7(1)	0.32

405
406 NB: Networks and sub-networks include OTUs and environmental factors. Di=Network diameter. De=Network density. Largest clique = size of
407 the largest clique(s) in the network, and in brackets, the number of them. Mod = Network modularity inferred using edge betweenness. [1]All
408 associations where picoplankton OTUs are involved (including nanoplankton); [2]Associations between picoplankton OTU only; [3]All associations
409 where nanoplankton OTUs are involved (including picoplankton); [4]Associations between nanoplankton OTU only; [5]All associations where
410 bacterial OTUs are involved (including protists); [6]Associations between bacterial OTU only; [7]All associations where protist OTUs are involved
411 (including bacteria); [8]Associations between protist OTU only. * Includes nodes and edges shared between pico- and nanoplankton. ** Includes
412 nodes and edges shared between bacteria and protists.

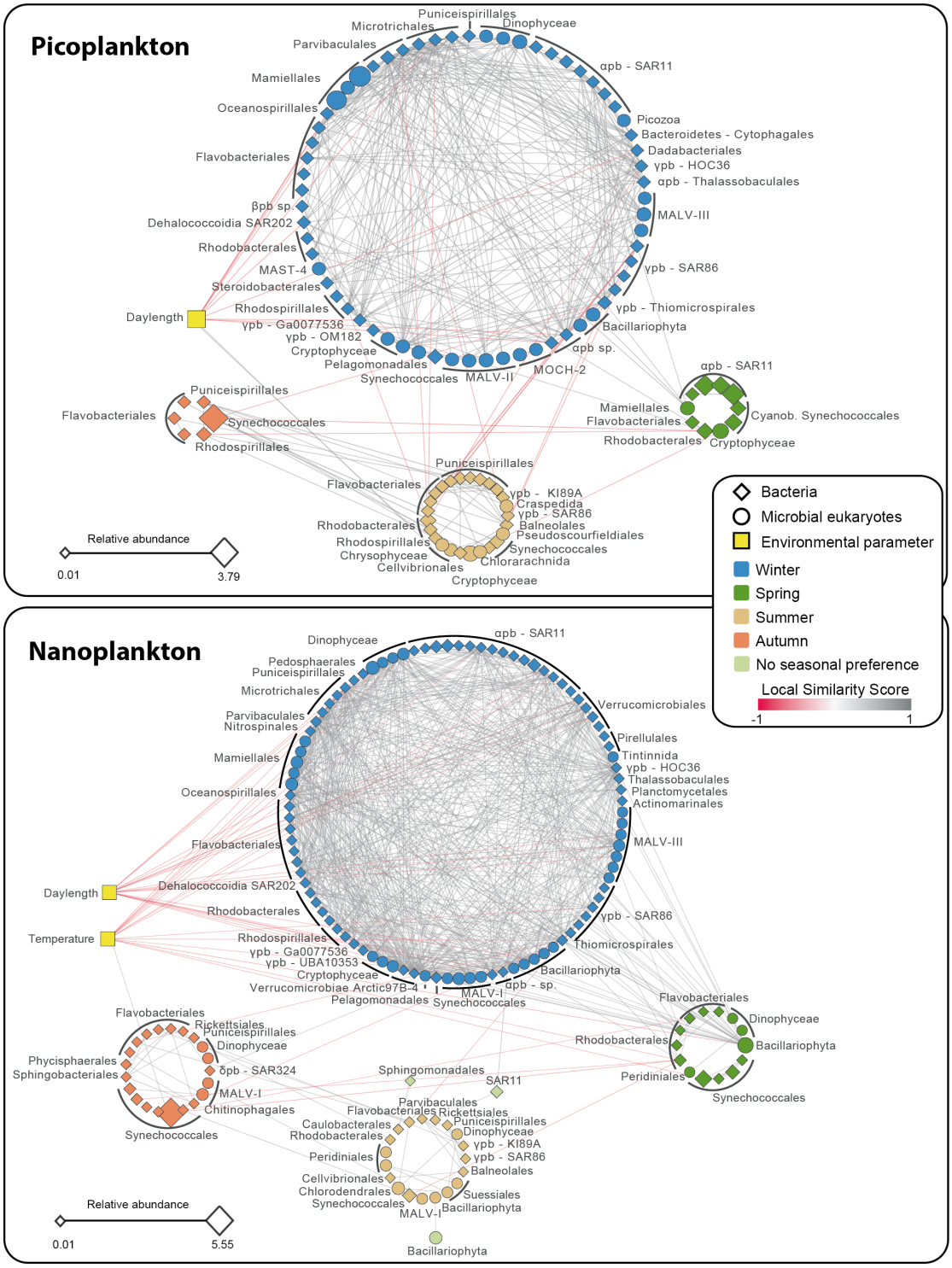

Figure 4. Pico- and nanoplankton core sub-networks. The shape of the nodes indicates bacteria (rhomboid) or microbial eukaryotes (circle), and the color of nodes represents species seasonal preferences, determined using the indicator value ($p<0.05$). The color of the edges

419 indicates if the association is positive (grey) or negative (red). Node size indicates OTU relative
420 abundance from the core microbiota.
421
422 **Table 4.** Core associations within and between taxonomic domains and size fractions.

Network	Association type[1]	# Associations
Core network	Total	1,411
	Bacteria - Bacteria	767 (54%)
	Bacteria - Protist	433 (31%)
	Protist - Protist	161 (11%)
	Environmental factor - Bacteria	36 (3%)
	Environmental factor - Protist	14 (1%)
Picoplankton subnetwork	Total	378
	Bacteria - Bacteria	241 (64%)
	Bacteria - Protist	94 (25%)
	Protist - Protist	31 (8%)
	Environmental factor - Bacteria	12 (3%
	Environmental factor - Protist	0 (0%)
Nanoplankton subnetwork	Total	791
	Bacteria - Bacteria	394 (50%)
	Bacteria - Protist	246 (31%)
	Protist - Protist	113 (14%)
	Environmental factor - Bacteria	24 (3%)
	Environmental factor - Protist	14 (2%)

423 [1] "Bacteria – Bacteria" indicates associations between two bacterial OTUs. "Protist – Protist" are associations between two unicellular eukaryotes
424 and "Bacteria – Protist" are associations between one eukaryote and one bacterial OTU. "Environmental factor – Protist" and "Environmental
425 factor – Bacteria" are associations between an environmental factor and a eukaryotic or bacterial OTU.
426

427 *Network seasonality*

428 The indicator value (IndVal) was used to infer the seasonal preference of core OTUs.
429 Most of the core OTUs (98%; 254 out of 259 OTUs) showed a clear preference for one
430 of the four seasons, pointing to a marked seasonality in the core microbiota (**Figure 4;**
431 **Table 5; Tables S4 & S5**). Winter had the highest quantity of core OTUs and the
432 highest network connectivity (average degree ~13), compared to the other seasons
433 (average degrees ~2 – ~6) [**Figure 4**; **Table 5**]. The average path length was larger in
434 the core network compared to a random network of the same size (**Table 3**). Yet, all
435 sub-networks associated with size fractions and seasons (**Table 5**) had shorter path
436 lengths than the random network,

437 that nodes tended to be connected within seasons and size fractions. This was also
438 supported by an increase in network density when comparing the core network (**Table**
439 **3**) and the core network subdivided into seasons (**Table 5**), against the core network
440 subdivided into both seasons and size fractions (**Table 5**). The five OTUs that did not
441 show any seasonal preference, among them SAR11 Clades Ia & II, showed high to
442 moderate abundances but had a low number of associations to other OTUs (**Tables S4,**
443 **S5, S6**). Thus, network connectivity in the BBMO appears to be heterogeneous over
444 time, peaking in winter and remaining low in the other seasons.
445

446 **Table 5:** Subnetworks including core OTUs displaying seasonal preference.
447

	Sub-network	Number of OTUs	Edges	Di.	De.	Average degree	Average path length	Average clustering coefficient	Largest clique (#)	Mod.
All	Winter	156	1,175	7	0.10	15.1	2.62	0.54	13(4)	0.19
	Spring	19	16	4	0.09	1.7	1.56	0.44	4(1)	0.75
	Summer	41	56	7	0.07	2.7	2.90	0.49	6(1)	0.53
	Autumn	26	25	3	0.08	1.9	1.59	0.46	4(2)	0.73
Pico	Winter	63	286	6	0.15	9.1	2.35	0.53	9(4)	0.10
	Spring	8	5	3	0.18	1.2	1.50	0.00	2(5)	0.56
	Summer	25	36	5	0.12	2.9	2.20	0.41	6(1)	0.23
	Autumn	5	3	2	0.30	1.2	1.25	0.00	2(3)	0.44
Nano	Winter	92	658	6	0.16	14.3	2.40	0.61	13(4)	0.04
	Spring	11	11	4	0.20	2.0	1.59	0.57	4(1)	0.56
	Summer	13	17	3	0.22	2.6	1.70	0.65	4(1)	0.50
	Autumn	17	18	3	0.13	2.1	1.35	0.56	4(2)	0.60

448 NB: Subnetworks include OTUs only. Di=Network diameter. De=Network density. Largest clique = size of the largest clique(s) in the network,
449 and in brackets, the number of them. Mod = Network modularity inferred using edge betweenness.
450

451 *Groups of highly associated OTUs*

452 Within the core network, we identified groups that were more connected to each other
453 than to the rest of the network (called modules). These groups of OTUs may indicate
454 recurring associations that are likely important for the stability of ecosystem function.
455 We identified 12 modules in both the pico- and nanoplankton subnetworks (**Table S7**).
456 Modules tended to include OTUs from the same season (**Table S8**), with main modules
457 (i.e. MCODE score >4) including OTUs predominantly associated with winter,
458 summer, and autumn (**Figure 5**). Overall, winter modules prevailed (5 out of 7) among

459 the main modules (**Figure 5**), while modules with scores ≤ 4 did not tend to be
460 associated with a specific season (**Table S8**). Two main winter modules had members
461 that were negatively correlated to temperature and daylength (**Figure 5**; Modules 1 and
462 4, nanoplankton).

463 The total relative sequence abundance of core OTUs included in modules was
464 ~24% (proportional to the resident microbiota), while the total abundance of individual
465 modules ranged between ~6% and ~0.3% (**Table S7**). In turn, the relative abundance
466 of core OTUs included in modules ranged between 0.01% and ~2% (**Table S8**). In most
467 modules, a few OTUs tended to dominate the abundance, although there were
468 exceptions, such as module 4 of the picoplankton, where all SAR11 members featured
469 abundances >1% (**Table S8**). In addition, several OTUs within modules had relatively
470 low abundances (**Table S8**), supporting modules as a real feature of the network and
471 not just the agglomeration of abundant taxa.

472

473 *Central OTUs*

474 Biological networks typically contain nodes (i.e. OTUs) that hold more "central"
475 positions in the network than others [22]. Even though the ecological role of these hub
476 and connector OTUs is unclear, it is acknowledged that they could reflect taxa with
477 important ecological functions [22]. There is no universal definition for hub or
478 connector OTUs, yet, in this work, we have used stringent thresholds to determine them
479 *ad hoc* (see Methods). We have identified 13 hub-OTUs that were associated with
480 winter or spring (**Table 6**). Hubs did not include highly abundant OTUs, such as
481 *Synechococcus* or SAR11 (**Table 6**), but instead, they included several OTUs with
482 moderate-low abundance (<1%) and high degree (ranging between 26-60) [**Table 6**].
483 For example, the Gammaproteobacteria OTU bn_000226 had a relative abundance of

484 0.04% and a degree of 60 **(Table 6)**. Hubs included other moderately abundant OTUs,
485 such as the eukaryotic picoalgae *Bathycoccus,* which was abundant in winter, as well
486 as an unidentified dinoflagellate (**Table 6**).

487 We identified a total of 18 connector OTUs (featuring relatively low degree and
488 high centrality), which were predominantly associated with summer (5 out of 18) or
489 autumn (6 out of 18), contrasting with hub OTUs, which were associated mostly with
490 winter and spring (**Table 6**). Connectors may be linked to the seasonal transition
491 between main community states (**Figure 1 C & D**) and included several abundant
492 OTUs belonging to *Synechococcus* and SAR11 (**Table 6**). In particular, the SAR11
493 OTU bp_000007 displayed a relatively high abundance (1.4%), but a degree of 3
494 (relatively low) and a betweenness centrality of 0.6 (relatively high). In contrast, two
495 protist OTUs displayed low-moderate abundances (ep_00269, Chrysophyceae,
496 abundance 0.04% and en_00161, Syndiniales, abundance 0.4%), low degree <4, but a
497 high betweenness centrality (>0.8; **Table 6**).

498

499 **Table 6.** Central OTUs

OTU	Class	Lowest rank taxonomy	Relative Abundance (%)[1]	Degree	Betweenness Centrality	Closeness Centrality	Season
Hubs							
en_00092	Mamiellophyceae	*Bathycoccus*	0.51	42	0.04	0.42	Winter
en_00119	Dinophyceae	-	0.41	50	0.03	0.42	Winter
bp_000037	Alphaproteobacteria	Parvibaculales_OCS116	0.31	45	0.08	0.43	Winter
bp_000039	Gammaproteobacteria	SUP05_cluster	0.28	29	0.12	0.41	Spring
bn_000039	Gammaproteobacteria	SUP05_cluster	0.21	42	0.17	0.44	Spring
bn_000037	Alphaproteobacteria	Parvibaculales_OCS116	0.20	40	0.05	0.42	Spring
bp_000059	Gammaproteobacteria	SAR86	0.20	24	0.09	0.40	Spring
ep_00070	Cryptophyceae	Cryptomonadales_X	0.13	40	0.04	0.42	Winter
bn_000059	Gammaproteobacteria	SAR86	0.12	24	0.03	0.40	Spring
bn_000102	Alphaproteobacteria	Nisaeaceae_OM75	0.09	26	0.03	0.38	Winter
bp_000193	Alphaproteobacteria	-	0.06	37	0.03	0.40	Winter
bn_000170	Acidimicrobiia	Sva0996_marine_group	0.06	59	0.06	0.44	Winter
bn_000226	Gammaproteobacteria	HOC36	0.04	60	0.06	0.43	Winter
Connectors							
bp_ 000001	Oxyphotobacteria	*Synechococcus* (CC9902)	3.79	5	0.05	0.30	Autumn
bp_ 000002	Alphaproteobacteria	SAR11 Clade_Ia	2.26	2	0.40	0.56	Spring
bp_ 000004	Alphaproteobacteria	SAR11 Clade_Ia	2.02	3	0.15	0.63	NA
bp_ 000007	Alphaproteobacteria	SAR11 Clade_Ia	1.38	3	0.60	0.71	NA
bp_ 000008	Alphaproteobacteria	SAR11 Clade_Ia	1.15	3	0.15	0.63	NA
bn_ 000008	Alphaproteobacteria	SAR11 Clade_Ia	0.68	5	0.03	0.27	Winter

en_ 00059	Chlorodendrophyceae	*Tetraselmis*	0.66	4	0.05	0.26	Summer
bn_ 000020	Oxyphotobacteria	-	0.56	3	0.60	0.67	Autumn
en_ 00161	Syndiniales	Syndiniales-Group-I-Clade-4_X	0.42	4	0.80	0.75	Autumn
bn_ 000018	Oxyphotobacteria	*Prochlorococcus* MIT9313	0.41	5	0.04	0.24	Winter
bn_ 000054	Alphaproteobacteria	Puniceispirillales_SAR116	0.11	4	0.14	0.40	Autumn
bn_ 000062	Alphaproteobacteria	Puniceispirillales_SAR116	0.08	3	0.55	0.50	Autumn
bn_ 000077	Rhodothermia	*Balneola*	0.07	3	0.17	0.32	Summer
bn_ 000112	Gammaproteobacteria	KI89A	0.06	4	0.53	0.48	Summer
bn_ 000156	Alphaproteobacteria	Parvibaculales_PS1	0.05	4	0.14	0.40	Summer
bn_ 000281	Bacteroidia	Sphingobacteriales_NS11-12	0.05	5	0.16	0.44	Autumn
bn_ 000221	Alphaproteobacteria	Puniceispirillales_SAR116	0.04	5	0.05	0.30	Winter
ep_ 00269	Chrysophyceae	Clade-I_X	0.04	2	1.00	1.00	Summer

[1] Proportional to the resident microbiota

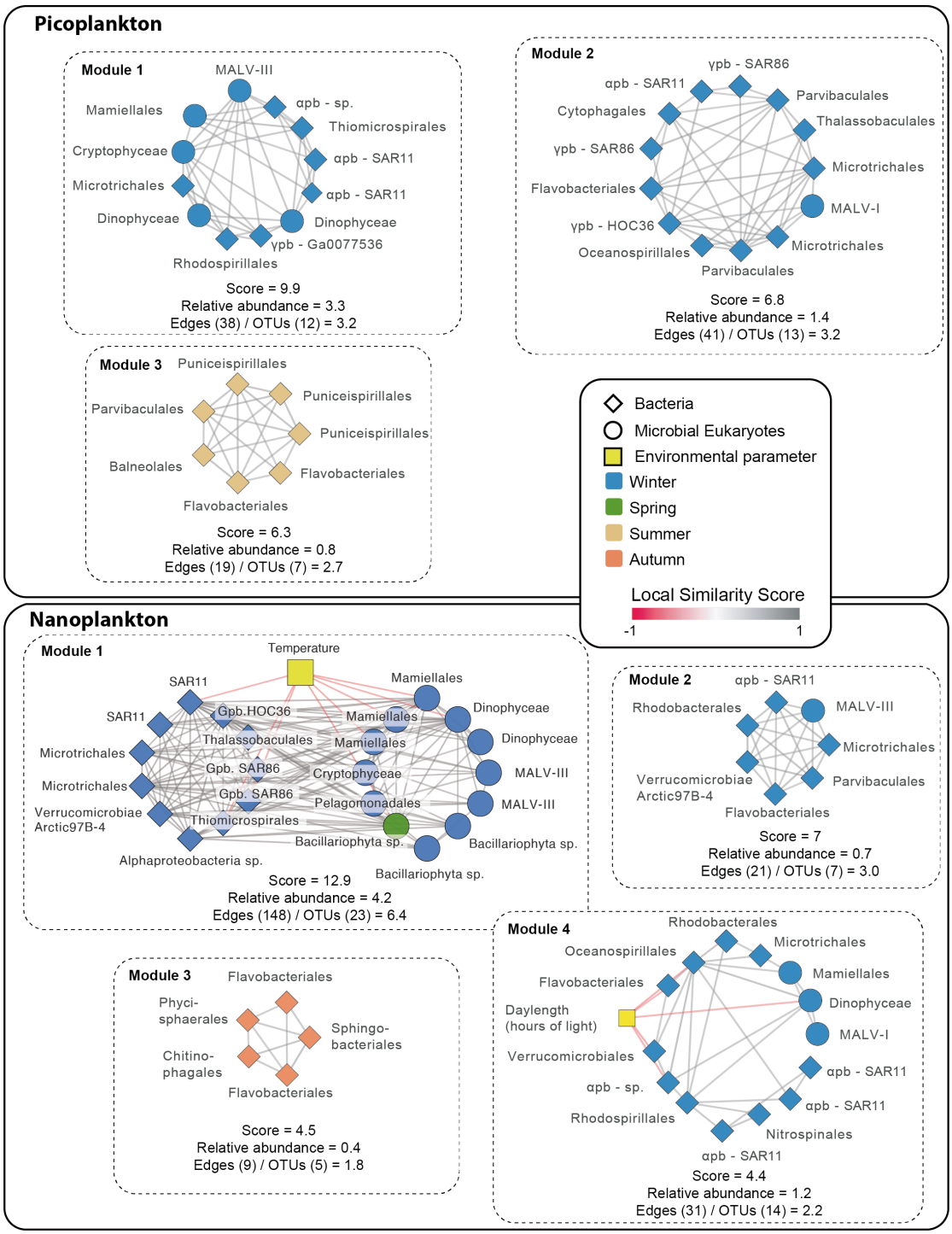

Figure 5. Main modules in the core network. Modules with MCODE score >4 are shown for picoplankton (upper panel) and nanoplankton (lower panel). For each module, the MCODE score and relative amplicon abundance of the taxa included in it (as % of the resident microbiota) are indicated. In addition, the numbers of edges and OTUs within the modules are shown as edges/OTUs; this quotient estimates the average number of edges per OTU within the different modules. The edges represent correlations with |LS| > 0.7, |ρ|>0.7, P<0.001 and Q<0.001. The color of the edges indicates positive (grey) or negative (red) associations. The shape of nodes

510 indicates bacteria (rhomboid) or microbial eukaryotes (circle), and the color of nodes represents
511 species seasonal preferences, determined using the indicator value ($p<0.05$). pb =
512 Proteobacteria
513
514

515 **DISCUSSION**

516 Identifying the most important microbes for the functioning of the ocean ecosystem is
517 a challenge, which can be addressed by delineating core microbiotas [4]. Recognizing
518 the most abundant and widespread microbes in the ocean is a step towards knowing the
519 core microbiota. However, this does not take into account the importance that both
520 microbial interactions and microbes with moderate or low abundance may have for the
521 functioning of ecosystems [4, 29, 38]. Considering potential interactions when
522 delineating core microbiotas may not only allow identifying moderate/low abundance
523 taxa that may have important roles in the community but could also allow excluding
524 taxa that are present in several locations but that may not have an important role for
525 community function (e.g., dormant cells or cells being dispersed [8]). Here, we have
526 delineated and analyzed the core microbiota of a coastal ecosystem-based on 10 years
527 of occurrence data considering possible interactions.

528 To detect the core microbiota, we first identified the resident OTUs, that is,
529 those that occur >30% of the time (i.e. >36 out of 120 months) over a decade. This
530 threshold was selected as it allows for seasonal OTUs that would be present recurrently
531 in at least one season. Analysis of the resident OTU dynamics indicated a clear
532 seasonality (**Figure 1 C-D**), and that the measured environmental factors could explain
533 ~45% of the resident microbiota variance. The main environmental drivers were
534 temperature and daylength, which is consistent with previous works from the same
535 time-series (BBMO) [34, 39, 40]. These values are lower than what has been reported

536 for bacteria in the English Channel, where daylength explains ~65% of community
537 variance [17], and higher than what has been reported for entire communities in the
538 time-series SPOT (California, 31%) [41] or SOLA (the Mediterranean Sea, ~130 km
539 from BBMO; 7-12%) [42]. Daylength may be more important in the English Channel
540 as it has a more pronounced annual variation than at BBMO, whereas the measured
541 differences could reflect a higher coupling of the resident OTUs with environmental
542 variation in BBMO than in SOLA or SPOT. SOLA is characterized by the occasional
543 winter storms that bring nutrients from the sediments to the water column as well as by
544 the freshwater inputs from nearby rivers during flash floods [43], and this could
545 partially explain the differences with BBMO. The importance of daylength and
546 temperature for community dynamics was reflected by niche analyses, which identified
547 two main niches associated with summer and winter at the BBMO, to which ~50% of
548 the resident OTUs were associated (**Figure 1 E-F**). Other resident OTUs likely have
549 spring and fall niches as indicated by **Figure 1 C-D**, yet these niches cannot be detected
550 with the used null model analysis, as their preferred temperatures or daylengths will not
551 depart significantly from the randomized mean.

552 Based on the resident OTUs, we built networks to define the core microbiota.
553 We identified a total of 259 core OTUs (182 bacteria and 77 protists) that represented
554 64% of the abundance of the resident microbiota and that showed seasonal variation.
555 We could only find supporting evidence from the literature (PIDA database) [21] for
556 85 associations of the core (6 %), indicating that most of them still need to be validated
557 with direct observation or experimentally. This is not surprising, as the most studied
558 hosts in PIDA are protists from the micro-plankton (>20 µm cell size), which are mostly
559 absent from our pico- and nanoplankton networks. Also, PIDA does not cover Bacteria-
560 Bacteria associations. Nevertheless, the detected core OTUs from BBMO represent a

561 fraction of the core microbiota at this site, since larger microbial size fractions were not
562 sampled. Including these larger size fractions would expand the composition of the core
563 and could unveil additional patterns. For example, in a global ocean network including
564 size fractions >20 µm cell size, protists or small multicellular eukaryotes dominated the
565 interactome [26].

566 Alpha-/Gammaproteobacteria, Bateroidia, Acidimicrobiia were the main
567 bacterial groups in the core, including also common marine taxa, such as
568 *Synechococcus* or SAR11. The main protists in the core included Syndiniales
569 (parasites), Dinoflagellates, Mammiellales (*Micromonas* and *Bathycoccus*), and
570 diatoms. These taxa are likely the most important in sustaining ecosystem function at
571 BBMO, and probably have similar importance in other coastal areas. Other studies have
572 reported important roles in marine association networks for SAR11 and *Synechococcus*
573 [31, 44]. Syndiniales, Haptophytes, and Dinoflagellates dominated networks in terms
574 of the number of nodes and edges at SPOT, while Mamiellales (*Micromonas* &
575 *Bathycoccus*) and diatoms also had relevant roles [41]. Syndiniales, Dinoflagellates,
576 and Diatoms were also predominant in global ocean networks, which is coherent with
577 our results [26].

578 Bacteria-Bacteria associations were the most abundant (54%) in the core
579 BBMO microbiota, followed by Bacteria-Protists (31%) and Protist-Protist (11%)
580 associations. Associations tended to occur among bacteria or protists, rather than
581 between them, in the English Channel time-series [17]. However, the study used
582 microscopy to determine protist community composition, while it used 16S-rRNA gene
583 data for analyzing bacteria communities and this might explain the limited number of
584 connections between protists and bacteria. Most associations occurred among protists
585 in a global-ocean network that included a broad range of microbial size-fractions [26].

586 This suggests that time-series analyses including larger size-fractions may determine a
587 higher proportion of associations among protists, which may turn out to be prevalent.
588 The core network had "small world" properties (that is, high clustering
589 coefficient and relatively short path lengths) [37] when compared to randomized
590 networks (**Table 3**) or particular subnetworks from size fractions or specific seasons
591 (**Table 5**). The small-world topology is characteristic of many different types of
592 networks [45], including marine microbial temporal or spatial networks [23, 26, 30,
593 31]. Some of our network statistics were similar to those obtained at SPOT [23, 30], in
594 particular the averages of degree, clustering coefficient, and path length (**Table 3**).
595 Furthermore, the BBMO network had an average path length similar to a global ocean
596 network [26] and also, similarly to this network, the node degree of the BBMO core
597 members was independent of their relative abundances, showing that the associations
598 between core OTUs were not merely a consequence of high prevalence and abundance.
599 The BBMO core network had a clustering coefficient that was ten times larger
600 than that of an Erdős–Rényi random network of the same size (**Table 3**), which agrees
601 with what was observed at SPOT [23, 30]. The large proportion of positive associations
602 in BBMO networks (~95%) was in agreement with results from other temporal [23, 41]
603 or large-scale spatial [26] microbiota analyses, where positive associations were also
604 predominant (~70-98%), although these values include taxa that are not necessarily part
605 of the core. This suggests that interactions such as syntrophy or symbiotic associations
606 are more important than competition in marine microbial systems and that these types
607 of associations may underpin marine ecosystem function. These findings are also
608 coherent with a recent large-scale literature survey that found that ~47% of the validated
609 associations between protists and bacteria are symbiotic [21]. Nevertheless, it is also
610 possible that common sampling strategies and methodological approaches do not detect

611 a substantial fraction of negative associations. For example, while positive correlations
612 in taxa abundance pointing to positive interactions may be easier to detect, negative
613 associations may be missed due to plummeting species abundances that would prevent
614 establishing significant correlations, or to a delay between the increase and decrease in
615 abundance of interacting taxa that are not synchronized with sampling time. Future
616 studies adapting the sampling scheme to the timing of interactions (e.g., daily or weekly
617 sampling) and the use of other approaches apart from taxa abundances, such as analyses
618 of single-cell genomic data to determine protistan predation, or controlled experiments,
619 will likely generate new insights on negative microbial interactions.

620 The relatively high clustering coefficient of the core network (compared to a
621 random network) and its short path length indicate that most OTUs are connected
622 through < 3 intermediary OTUs. It has been shown that a large proportion of strong
623 positive associations, as in the BBMO core network, may destabilize communities due
624 to positive feedbacks between species [46]. When a species decreases in abundance as
625 a response to environmental variation, it may pull others with it, generating a cascade
626 effect propagated by the many positive associations in the network. Accordingly, the
627 change of abundance in specific OTUs in one section of the network could affect OTUs
628 in other network sections not necessarily affected directly by the environmental
629 variation. This cascade effect may help to explain a paradox: environmental variables
630 affect the structure of marine microbial communities and consequently association
631 networks. Yet, our and others' results [17, 18, 23, 26, 30-32] have reported a limited
632 number of associations between environmental variables and network nodes (OTUs).
633 Environmental heterogeneity might affect network structure by acting on a small subset
634 of nodes (OTUs), which would then influence other nodes through cascading

635 interactions facilitated by the highly interconnected nature of the networks as well as
636 positive feedbacks promoted by the high proportion of positive associations [46].

637 If OTUs susceptible to environmental variation are also highly connected, then
638 their effect on the entire network structure may be larger. In line with this, we found
639 that the connectivity of OTUs associated with environmental variables at BBMO (49
640 OTUs out of 259) had a mean degree of ~25 (SD ~14), while for all the 259 OTUs of
641 the core network, the mean degree was ~11 (SD ~13). The seasonal dynamics of the
642 BBMO microbiota may partially be driven by a subset of OTUs that vary with
643 environmental factors (e.g. temperature, daylength). These may exert a destabilizing
644 influence over the entire community over time, promoting the annual turnover of
645 communities and networks.

646 Most core OTUs (98%) showed a clear preference for one season. Interestingly,
647 the distribution of core OTUs among the seasons was uneven, with 61% of these OTUs
648 showing a winter preference. Network connectivity at BBMO was correspondingly
649 heterogeneous between seasons, peaking in winter and remaining low in the other
650 seasons. Specifically, the winter subnetwork included ~92% of the seasonal edges. This
651 indicates that winter associations are not only specific (i.e. they do not tend to change
652 partners), but they also have a relatively high recurrence (otherwise, winter networks
653 would be smaller). A higher similarity between winter communities when compared to
654 other seasons was also indicated by our ordination analyses of the resident OTUs
655 (**Figure 1**), as well as by studies of the entire protist community at BBMO [34] or whole
656 community analyses at SPOT [23].

657 The structure of communities is determined by the interplay of selection,
658 dispersal, speciation, and ecological drift [47]. Our results indicate that selection, a
659 deterministic process, is stronger in winter, leading to winter sub-communities that tend

660 to be more similar between each other than to communities from other seasons. Given
661 that we have removed edges associated with the measured environmental variables, we
662 do not expect that the identified edges between winter OTUs represent selection
663 associated to these variables (e.g. low temperature). Consequently, winter edges may
664 represent associations linked to unmeasured variables or ecological interactions that
665 may be more likely to develop during winter due to stronger environmental selection.
666 Due to weaker selection in other seasons species occurrence would display less
667 recurrent (or more random) patterns, preventing specific associations to be formed. This
668 also suggests that ecological redundancy changes over time, and is lower in winter
669 compared to the other seasons (even though the number of OTUs is larger in winter).
670 A reduction in redundancy may also promote strong ecological interactions in winter.

671 The existence of subsets of species that interact more often between themselves
672 than with other species (modules), is characteristic of biological networks, and can
673 contribute to overall network stability [48, 49]. Modules can represent divergent
674 selection, niches, the clustering of evolutionary closely related species or co-
675 evolutionary units [50, 51]. Modules in the core BBMO network (total 12) included
676 positive associations between diverse taxa, and could represent divergent selection,
677 driven by unmeasured environmental variables, or examples of syntrophic or symbiotic
678 interactions between microbes from different taxonomic groups.

679 Most BBMO modules included diverse lifestyles (heterotrophs, mixotrophs,
680 phototrophs, parasites), similar to what has been observed at SPOT [41]. Yet, a number
681 of modules appeared to be predominantly heterotrophic or autotrophic (**Table S8**).
682 Some modules included OTUs from the same species, such as Module 4 in the
683 picoplankton, which included several SAR11 Clade I OTUs, and Module 7 of the
684 nanoplankton, which included several *Synechococcus* OTUs. These modules could

685 reflect similar niches, associated with unmeasured variables, or the dependence on
686 metabolites produced by other organisms (auxotrophy). There is evidence of
687 auxotrophy for both SAR11 (e.g. thiamin, glycine)[52-54] and *Synechococcus* (e.g.
688 cobalamin) [55]. Recently it has been observed in co-culture experiments that
689 *Prochlorococcus* may fulfill some metabolic requirements of SAR11, promoting the
690 growth of the latter in a commensal relationship [56]. In our analyses of the BBMO
691 core microbiota, we did not find strong associations between SAR11 and
692 *Prochlorococcus* or the more abundant relative, *Synechococcus*. Yet, SAR11 formed
693 strong associations with a plethora of taxa with which could potentially have
694 commensal relationships.

695 The overall importance of the observed modules was indicated by the total
696 abundance of their constituent OTUs (24% of the reads compared to the resident
697 microbiota). Most of the modules at BBMO were associated with a single season,
698 suggesting that they reflect seasonal niches. Since these modules were inferred over 10
699 years, they represent recurrent network features. Chafee et al. [57] also identified
700 season-specific modules in a 2-year time series in the North Sea (Helgoland), including
701 samples taken weekly or bi-weekly. These modules were much larger than ours, and
702 they may also include environmentally-driven edges. Nevertheless, the Helgoland
703 modules seem to be driven by eutrophic (spring & summer) vs. oligotrophic (autumn
704 & winter) conditions in this location. In contrast, the BBMO modules, displayed weaker
705 correlations with nutrients and seem to be influenced by temperature and daylength
706 (**Figure 5**). Differences in the sampling scheme between Helgoland and BBMO
707 ((bi)weekly vs. monthly) as well as between both locations (different seas and latitudes,
708 affecting temperature and daylength) may explain these differences.

709 Keystone species have a high influence in ecosystems relative to their
710 abundance [58]. Network analyses may help to identify them [24, 59], yet, there is no
711 clear consensus of what network features are the best unequivocal indicator of keystone
712 species [60-62]. Therefore, we focused on identifying central OTUs (hubs or
713 connectors) that may be important for ecosystem function [22, 24] and could represent
714 keystone species. We identified 13 hubs in the BBMO core network with moderate-low
715 abundances (<1%) and high degree (26-60) that were associated with winter or spring.
716 These moderate-low abundance OTUs may affect nutrient cycling directly [63] or
717 indirectly, by affecting other OTUs with higher abundance. The putative stronger
718 selection exerted by low temperatures and short daylengths during winter and early
719 spring, as compared to summer and autumn, may lead to a higher species recurrence
720 [34], larger networks, and possibly, more hubs. An OTU of the abundant picoalgae
721 *Bathycoccus* (en_00092) was identified as a winter hub, which is consistent with
722 reported *Bathycoccus* abundance peaks in late winter (February-March) in both BBMO
723 [64] and the nearby station SOLA [42]. This *Bathycoccus* hub may be associated with
724 diverse taxa, such as prokaryotes that may benefit from algal exudates [65] or even via
725 mixotrophy [66]. In agreement with this, out of the 42 associations of this hub OTU,
726 25 were with bacteria and the rest with protists.

727 In contrast to hubs, connector OTUs were predominantly associated with
728 warmer waters, that is, summer and autumn, and may represent transitions in
729 community states. This was consistent with the associations observed in an abundant
730 *Synechococcus* connector OTU (bp_000001, **Table 6**). This OTU was predominant in
731 summer-autumn, in agreement with previous BBMO reports [36, 67], but it was
732 associated with other OTUs from spring (negative association with bp_000017), winter
733 (negative association with bp_000039), summer (positive association with bp_000087,

734 bp_000012) and autumn (positive association with bp_000022), thus likely holding a
735 central position in the network. Another abundant spring connector OTU (SAR11 Clade
736 Ia, bp_000002), featured only two connections to spring (positive association with
737 bp_000007) and summer (positive association with bp_000046) OTUs.
738

739 **CONCLUSION**

740 Our decade-long analysis of the dynamics of a microbiota populating a time-series in
741 the Mediterranean Sea allowed us to determine the interconnected core microbiota,
742 which likely includes several microbes that are important for the functioning of this
743 coastal ecosystem. We found a relatively small core microbiota that displayed seasonal
744 variation, with a heterogeneous distribution of associations over different seasons,
745 indicating different degrees of recurrence and selection strength over the year. Future
746 analyses of other core marine microbiotas will determine how universal are the patterns
747 found in BBMO. These studies will be crucial to determine potential long-term effects
748 of climate change on the architecture of the interaction networks that underpin the
749 functioning of the ocean ecosystem.

750 **METHODS**

751 *Study site and sampling*

752 Surface water (~1 m depth) was sampled monthly from January 2004 to December
753 2013 at the Blanes Bay Microbial Observatory (BBMO) in the Northwestern
754 Mediterranean Sea (41º40'N, 2º48'E) [**Figure 1A**]. The BBMO is an oligotrophic
755 coastal site ~1 km offshore with ~20 m depth and with limited riverine or human
756 influence [36]. Seawater was pre-filtered with a 200 µm nylon mesh and then
757 transported to the laboratory in 20 L plastic carboys and processed within 2 hours.
758 Microbial plankton from about 6 L of the pre-filtered seawater was separated into two

759 size fractions: picoplankton (0.2-3 µm) and nanoplankton fraction (3-20 µm). To
760 achieve this, the seawater was first filtered through a 20 µm nylon mesh using a
761 peristaltic pump. Then the nanoplankton (3-20 µm) was captured on a 3 µm pore-size
762 polycarbonate filter. Subsequently, a 0.2 µm pore-size Sterivex unit (Millipore,
763 Durapore) was used to capture the picoplankton (0.2-3 µm). Sterivex units and 3 µm
764 filters were stored at -80 ºC until further processed. The sequential filtering process
765 aimed to capture free-living bacteria and picoeukaryotes in the 0.2-3 µm size fraction
766 (picoplankton), and particle/protist-attached bacteria or nanoeukaryotes in the 3-20 µm
767 fraction (nanoplankton). The 3µm filter was replaced if clogging was detected; DNA
768 from all 3µm filters from the same sample were extracted together.

769 A total of 15 contextual abiotic and biotic variables were considered for each
770 sampling point: Daylength (hours of light), Temperature (°C), Turbidity (estimated as
771 Secchi disk depth [m]), Salinity, Total Chlorophyll a [Chla] (µg/l), PO_4^{3-} (µM), NH_4^+
772 (µM), NO_2^- (µM), NO_3^- (µM), SiO_2 (µM), abundances of Heterotrophic prokaryotes
773 [HP] (cells/ml), *Synechococcus* (cells/ml), Total photosynthetic nanoflagellates [PNF;
774 2-5µm size] (cells/ml), small PNF (2µm ; cells/ml) and, Heterotrophic nanoflagellates
775 [HNF] (cells/ml) [**Figure 1B**]. Water temperature and salinity were sampled *in situ* with
776 a SAIV A/S SD204 CTD. Inorganic nutrients (NO_3^-, NO_2^-, NH_4^+, PO_4^{3-}, SiO_2) were
777 measured using an Alliance Evolution II autoanalyzer [68]. Cell counts were done by
778 flow cytometry (heterotrophic prokaryotes, *Synechococcus*) or epifluorescence
779 microscopy (PNF, small PNF and HNF). See Gasol *et al.* [36] for specific details on
780 how other variables were measured. Environmental variables were z-score standardized
781 before running statistical analysis.

782

783 *DNA extraction, sequencing, and metabarcoding*

784 DNA was extracted from the filters using a standard phenol-chloroform protocol [69],
785 purified in Amicon Units (Millipore), and quantified and qualitatively checked with a
786 NanoDrop 1000 Spectrophotometer (Thermo Fisher Scientific). Eukaryotic PCR
787 amplicons were generated for the V4 region of the 18S rDNA (~380 bp), using the
788 primer pair TAReukFWD1 and TAReukREV3 [70]. The primers Bakt_341F [71] and
789 Bakt_806RB [72] were used to amplify the V4 region of the 16S rDNA. PCR
790 amplification and amplicon sequencing were carried out at the Research and Testing
791 Laboratory (http://rtlgenomics.com/) on the *Illumina* MiSeq platform (2x250 bp paired-
792 end sequencing). DNA sequences and metadata are publicly available at the European
793 Nucleotide Archive (http://www.ebi.ac.uk/ena; accession numbers PRJEB23788 for
794 18S rRNA genes & PRJEB38773 for 16S rRNA genes).

795 A total of 29,952,108 and 16,940,406 paired-end *Illumina* reads were produced
796 for microbial eukaryotes and prokaryotes respectively. Adapters and primers were
797 removed with Cutadapt v1.16 [73]. DADA2 v1.10.1 [74] was used for quality control,
798 trimming, and inference of Operational Taxonomic Units (OTUs) as Amplicon
799 Sequence Variants (ASVs). For both microbial eukaryotes and prokaryotes, the
800 Maximum number of expected errors (MaxEE) was set to 2 and 4 for the forward and
801 reverse reads respectively. No ambiguous bases (Ns) were allowed. Microbial
802 eukaryotic sequences were trimmed to 220 bp (forward) and 190 bp (reverse), while
803 prokaryotic sequences were trimmed to 225 bp (both forward and reverse reads). A
804 total of 28,876 and 19,604 OTUs were inferred for microbial eukaryotes and
805 prokaryotes respectively.

806 OTUs were assigned taxonomy using the naïve Bayesian classifier method [75]
807 together with the SILVA version 132 [76] database as implemented in DADA2.
808 Eukaryotic OTUs were also BLASTed [77] against the Protist Ribosomal Reference

809 database (PR^2, version 4.10.0; [78]). When the taxonomic assignments for the
810 eukaryotes disagreed between SILVA and PR^2, the conflict was resolved manually by
811 inspecting a pairwise alignment of the OTU and the closest hits from the two databases.
812 OTUs assigned to Metazoa, Streptophyta, nucleomorph, chloroplast, and mitochondria
813 were removed before further analysis. Archaea were removed from downstream
814 analyses as the used primers are not optimal for recovering this domain [79].

815 Each sample (corresponding to a specific gene, size fraction, and timepoint) was
816 subsampled with the *rrarefy* function from the R package *Vegan* [80] to 4,907 reads,
817 corresponding to the number of reads in the sample with the lowest sequencing depth,
818 to normalize for different sequencing depth between samples. OTUs present in <10%
819 of the samples were removed. After quality control and rarefaction, the number of
820 OTUs was 2,926 (1,561 bacteria, and 1,365 microeukaryotes; **Table 1**).

821 Due to a suboptimal sequencing of the amplicons, we did not use nanoplankton
822 samples of bacteria and protists from the period May 2010 to July 2012 (27 samples)
823 as well as March 2004 and February 2005. OTU read abundance for samples with
824 missing values were estimated using seasonally aware missing value imputation by
825 weighted moving average for time series as implemented in the R package *imputeTS*
826 [81].

827 Cell/particle dislodging or filter clogging during the sequential filtration process
828 may affect the taxonomic diversity observed in the different size fractions, with
829 nanoplankton DNA leaking into the picoplankton fraction, or picoplankton DNA
830 getting stuck in the nanoplankton fraction. To minimize the effects of cell/particle
831 dislodging or filter clogging on the diversity recovered from the different size fractions,
832 we calculated the sequence-abundance ratio for OTUs appearing in both pico- and
833 nano-plankton fractions. When the ratio exceeded 2:1, we removed the OTU from the

size fraction with the lowest number of reads. After subsampling and filtering the OTU tables were joined for each time point, and since the samples had been normalized to the same sequencing depth, we calculated the relative read abundance for the OTUs for each year and aggregated over the corresponding months along the 10 years for the resident microbiota. This means that the relative abundance for both domains and size fractions sums up to 1 for each month across ten years.

Resident microbiota

We defined *ad hoc* the resident microbiota as the set of OTUs present in >30% of the samples over 10 years (that is, present in >36 months, not necessarily consecutive). This value was chosen as it allows for seasonal OTUs, which may only be present 3-4 months each year, and still be considered as part of the resident microbiota. The residents included 355 eukaryotic and 354 bacteria OTUs (**Table 1**), and excluded a substantial amount of rare OTUs, which can cause spurious correlations during network construction due to sparsity [i.e. too many zeros] [22]. The relative abundance of the taxonomic groups included in the resident microbiota was fairly stable from year to year (**Figure 3**).

Environmental variation and resident OTUs

All possible correlations among the measured environmental variables and resident OTU richness and abundance were computed in R and plotted with the package *corrplot*. Only significant Pearson correlation coefficients were considered ($p<0.01$), and the p-values were corrected for multiple inference (Holm's method) using the function *rcorr.adjust* from the R package *RcmdrMisc*. Unconstrained ordination analyses were carried out using NMDS based on Bray Curtis dissimilarities between

859 samples including resident OTUs only. Environmental variables were fitted to the
860 NMDS using the function *envfit* from the R package *Vegan* [80]. Only variables
861 displaying a significant correlation ($p<0.05$) were considered. Constrained ordination
862 was performed using distance-based redundancy analyses (dbRDA) in *Vegan*,
863 considering Bray Curtis dissimilarities between samples including resident OTUs only.
864 The most relevant variables for constrained ordination were selected by stepwise model
865 selection using 200 permutations, as implemented in *ordistep* (*Vegan*). Ordinations
866 were plotted using the R package *ggplot2* and *ggord*. The amount of community
867 variance explained by the different environmental variables was calculated with *Adonis*
868 (Vegan) using 999 permutations. Resident OTUs displaying niche preference in terms
869 of Temperature and Daylength, the most important environmental variables, were
870 determined using the function *niche.val* from the R package *EcolUtils* with 1,000
871 permutations.
872
873 *Delineation of seasons*
874 Seasons were defined following Gasol *et al.* [36] with a small modification: months
875 with water temperature (at the sampling time) >17 °C and daylength >14 h d^{-1} were
876 considered to be summer. Months with water temperature <17 °C and < 11 h d^{-1} of
877 daylength were considered to be winter. Months with water temperature >17°C and
878 daylength <14 h d^{-1} were considered as autumn, while months with water temperature
879 <17°C and > 11 h d^{-1} of daylength were considered to be spring. The indicator value
880 [82] was calculated using the R package *labdsv* [83] to infer OTU seasonal preference.
881
882 *Core microbiota delineated using networks*

883 OTUs from the resident microbiota together with the 15 environmental variables were
884 used to construct association networks using extended Local Similarity Analysis
885 (eLSA) [84-86]. eLSA was run on the OTU table with subsampled reads with default
886 normalization: a z-score transformation using the median and median absolute
887 deviation. P-value estimations were run under a mixed model that performs a random
888 permutation test of a co-occurrence only if the theoretical p-values for the comparison
889 are <0.05. Bonferroni false discovery rate (q) was calculated for all edges based on the
890 p-values using the *p.adjust* package in R.

891 To detect environmentally-driven associations between OTUs induced by the
892 measured environmental variables we used the program EnDED [87].
893 Environmentally-driven associations indicate similar or different environmental
894 preferences between OTUs and not ecological interactions. In short, EnDED evaluates
895 associations between two OTUs that are both connected to the same environmental
896 variable based on a combination of four methods: *Sign Pattern*, *Overlap, Interaction*
897 *Information,* and *Data Processing Inequality.* These methods use the sign (positive or
898 negative) and the duration of the association, the relative abundance of OTUs as well
899 as environmental parameters to determine if an association is environmentally-driven.
900 If the four methods agreed that an association was environmentally-driven, then it was
901 removed from the network. The initial number of edges was 199,937, of which 180,345
902 were OTU-OTU edges that were at least in one triplet with an environmental parameter.
903 In total 65,280 (~33%) edges in the network were identified as indirect by EnDED and
904 removed. Afterward, only edges representing the strongest associations (i.e., absolute
905 local similarity score $|LS| > 0.7$, Spearman correlation $|\rho| > 0.7$, $P<0.001$ and $Q<0.001$)
906 were retained for downstream analysis and are hereafter referred to as "core
907 associations". Those OTUs participating in core associations were defined as core

908 OTUs, although their involvement in ecological interactions need further experimental
909 validation. Both core associations and core OTUs constitute the "core network", which
910 also represents the core microbiota (both "core network" and "core microbiota" are
911 used indistinctively). The core network was randomized using the Erdős–Rényi model
912 [88], using 262 nodes and 1,411 edges.

913 For the core network, we calculated: 1) *Density:* quantifies the proportion of
914 actual network connections out of the total number of possible connections, 2)
915 *Transitivity* or *Clustering coefficient:* measures the probability that nodes connected to
916 a node are also connected, forming tight clusters, 3) *Average path length:* mean number
917 of steps (edges) along the shortest paths for all possible pairs of nodes in the network
918 (a low average path length indicates that most species in the network are connected
919 through a few intermediate species), 4) *Degree:* number of associations per node, 5)
920 *Betweenness centrality:* measures how often an OTU (node) appears on the shortest
921 paths between other OTUs in the network, 6) *Closeness centrality:* indicates how close
922 a node is to all other nodes in a network, 7) *Cliques:* refers to sets of interconnected
923 nodes where all possible connections are realized, 8) *Modularity:* measures the division
924 of a given network into modules (that is, groups of OTUs that are highly interconnected
925 between themselves).

926 The Degree, Betweenness centrality and Closeness centrality were used to
927 identify central OTUs using *ad hoc* definitions. "Hub" OTUs were those with a score
928 above the average for the three statistics and were normally among the top 25% in each
929 score [22, 62, 89]. Specifically, hub OTUs featured a degree >24, Betweenness
930 centrality >0.03 and Closeness centrality >0.3. Similarly, "connector" OTUs were
931 defined as those featuring a relatively low degree and high centrality and could be seen
932 as elements that connect different regions of a network or modules [50]. Connector

933 OTUs featured a degree <5, Betweenness centrality > 0.03 and Closeness centrality
934 >0.2. Network statistics were calculated with *igraph* in R [90] , Gephi [91] and
935 Cytoscape v3.6.1 [92]. Visualizations were made in Cytoscape v3.6.1. Modules in the
936 core network were identified with MCODE [93].
937
938
939 **DECLARATIONS**
940
941 ***Ethics approval and consent to participate***
942 *Not applicable*
943
944 ***Consent for publication***
945 *Not applicable*
946
947 ***Availability of data and materials***
948 DNA sequences and metadata are publicly available at the European Nucleotide
949 Archive (http://www.ebi.ac.uk/ena; accession numbers PRJEB23788 [18S rRNA
950 genes] & PRJEB38773 [16S rRNA genes]).
951
952 ***Competing interests***
953 The authors declare that they have no competing interests
954
955 ***Funding***
956 RL was supported by a Ramón y Cajal fellowship (RYC-2013-12554, MINECO,
957 Spain). IMD was supported by an ITN-SINGEK fellowship (ESR2-EU-H2020-MSCA-

ITN-2015, Grant Agreement 675752 [ESR2] to RL). This work was supported by the projects INTERACTOMICS (CTM2015-69936-P, MINECO, Spain to RL), MicroEcoSystems (240904, RCN, Norway to RL), MINIME (PID2019-105775RB-I00, AEI, Spain, to RL), ALLFLAGS (CTM2016-75083-R, MINECO to RM), MIAU (RTI2018-101025-B-I00, to JMG) and DEVOTES (grant agreement n° 308392, European Union to EG). It was further supported by Grup Consolidat de Recerca 2017SGR/1568 (Generalitat de Catalunya).

Authors' contributions

AKK & RL designed the study. JMG, RM organized sampling. VB, CRG & IF collected samples, extracted the DNA, and organized its sequencing. AKK, RL & ID analyzed the data, while JMG, RM, IF, CRG & EG, provided contextual ecological or environmental pre-processed data. AKK, MFMB & RL interpreted the results. AKK & RL wrote the manuscript. All authors contributed substantially to manuscript revisions. All authors read and approved the final manuscript.

Acknowledgements

We thank all members of the Blanes Bay Microbial Observatory sampling and analyses team. Bioinformatics analyses were performed at the MARBITS platform of the Institut de Ciències del Mar (ICM; http://marbits.icm.csic.es).

REFERENCES

1. Gitay H, Wilson JB, Lee WG. Species Redundancy: A Redundant Concept? Journal of Ecology. 1996; 84(1):121-124.
2. Louca S, Parfrey LW, Doebeli M. Decoupling function and taxonomy in the global ocean microbiome. Science. 2016; 353:1272-1277.

3. Galand PE, Pereira O, Hochart C, Auguet JC, Debroas D. A strong link between marine microbial community composition and function challenges the idea of functional redundancy. ISME J. 2018; 12(10):2470-2478.
4. Shade A, Handelsman J. Beyond the Venn diagram: the hunt for a core microbiome. Environ Microbiol. 2012; 14(1):4-12.
5. Little AEF, Robinson CJ, Peterson SB, Raffa KF, Handelsman J. Rules of Engagement: Interspecies Interactions that Regulate Microbial Communities. Annual Review of Microbiology. 2008; 62(1):375-401.
6. Lennon JT, Jones SE. Microbial seed banks: the ecological and evolutionary implications of dormancy. Nat Rev Microbiol. 2011; 9(2):119-130.
7. Singer E, Wagner M, Woyke T. Capturing the genetic makeup of the active microbiome in situ. ISME J. 2017; 11(9):1949-1963.
8. Mestre M, Höfer J. The Microbial Conveyor Belt: Connecting the Globe through Dispersion and Dormancy. Trends Microbiol. 2021; in press.
9. Turnbaugh PJ, Ley RE, Hamady M, Fraser-Liggett CM, Knight R, Gordon JI. The Human Microbiome Project. Nature. 2007; 449(7164):804-810.
10. Wirth R, Kádár G, Kakuk B, Maróti G, Bagi Z, Szilágyi Á, Rákhely G, Horváth J, Kovács KL. The Planktonic Core Microbiome and Core Functions in the Cattle Rumen by Next Generation Sequencing. Front Microbiol. 2018; 9(2285).
11. Rubio-Portillo E, Kersting DK, Linares C, Ramos-Esplá AA, Antón J. Biogeographic Differences in the Microbiome and Pathobiome of the Coral *Cladocora caespitosa* in the Western Mediterranean Sea. Front Microbiol. 2018; 9(22).
12. Sweet MJ, Bulling MT. On the Importance of the Microbiome and Pathobiome in Coral Health and Disease. Frontiers in Marine Science. 2017; 4(9).
13. Lurgi M, Thomas T, Wemheuer B, Webster NS, Montoya JM. Modularity and predicted functions of the global sponge-microbiome network. Nature communications. 2019; 10(1):992.
14. Björk JR, O'Hara RB, Ribes M, Coma R, Montoya JM. The dynamic core microbiome: Structure, dynamics and stability. bioRxiv. 2018.
15. Delgado-Baquerizo M, Oliverio AM, Brewer TE, Benavent-González A, Eldridge DJ, Bardgett RD, Maestre FT, Singh BK, Fierer N. A global atlas of the dominant bacteria found in soil. Science. 2018; 359:320-325.
16. Logares R, Deutschmann IM, Junger PC, Giner CR, Krabberød AK, Schmidt TSB, Rubinat-Ripoll L, Mestre M, Salazar G, Ruiz-González C *et al*. Disentangling the mechanisms shaping the surface ocean microbiota. Microbiome. 2020; 8(1):55.
17. Gilbert JA, Steele JA, Caporaso JG, Steinbruck L, Reeder J, Temperton B, Huse S, McHardy AC, Knight R, Joint I *et al*. Defining seasonal marine microbial community dynamics. ISME J. 2012; 6(2):298-308.
18. Chow CE, Sachdeva R, Cram JA, Steele JA, Needham DM, Patel A, Parada AE, Fuhrman JA. Temporal variability and coherence of euphotic zone bacterial communities over a decade in the Southern California Bight. ISME J. 2013; 7(12):2259-2273.
19. Worden AZ, Follows MJ, Giovannoni SJ, Wilken S, Zimmerman AE, Keeling PJ. Rethinking the marine carbon cycle: factoring in the multifarious lifestyles of microbes. Science. 2015; 347(6223):1257594.
20. Krabberød AK, Bjorbækmo MFM, Shalchian-Tabrizi K, Logares R. Exploring the oceanic microeukaryotic interactome with metaomics approaches. Aquat Microb Ecol. 2017; 79(1):1-12.

1034 21. Bjorbaekmo MFM, Evenstad A, Rosaeg LL, Krabberod AK, Logares R. The
1035 planktonic protist interactome: where do we stand after a century of research?
1036 ISME J. 2020; 14(2):544-559.
1037 22. Röttjers L, Faust K. From hairballs to hypotheses - biological insights from
1038 microbial networks. FEMS Microbiol Rev. 2018; 42(6):761-780.
1039 23. Chow CE, Kim DY, Sachdeva R, Caron DA, Fuhrman JA. Top-down controls
1040 on bacterial community structure: microbial network analysis of bacteria, T4-
1041 like viruses and protists. ISME J. 2014.
1042 24. Layeghifard M, Hwang DM, Guttman DS. Disentangling Interactions in the
1043 Microbiome: A Network Perspective. Trends Microbiol. 2017; 25(3):217-228.
1044 25. Fuhrman JA, Cram JA, Needham DM. Marine microbial community dynamics
1045 and their ecological interpretation. Nat Rev Microbiol. 2015; 13(3):133-146.
1046 26. Lima-Mendez G, Faust K, Henry N, Decelle J, Colin S, Carcillo F, Chaffron S,
1047 Ignacio-Espinosa JC, Roux S, Vincent F *et al*. Determinants of community
1048 structure in the global plankton interactome. Science. 2015;
1049 348(6237):1262073.
1050 27. Ponisio LC, Valdovinos FS, Allhoff KT, Gaiarsa MP, Barner A, Guimarães PR,
1051 Hembry DH, Morrison B, Gillespie R. A Network Perspective for Community
1052 Assembly. Frontiers in Ecology and Evolution. 2019; 7(103).
1053 28. Chaffron S, Rehrauer H, Pernthaler J, von Mering C. A global network of
1054 coexisting microbes from environmental and whole-genome sequence data.
1055 Genome Res. 2010; 20(7):947-959.
1056 29. Krabberod AK, Bjorbaekmo MFM, Shalchian-Tabrizi K, Logares R. Exploring
1057 the oceanic microeukaryotic interactome with metaomics approaches. Aquat
1058 Microb Ecol. 2017; 79(1):1-12.
1059 30. Cram JA, Xia LC, Needham DM, Sachdeva R, Sun F, Fuhrman JA. Cross-depth
1060 analysis of marine bacterial networks suggests downward propagation of
1061 temporal changes. ISME J. 2015; 9(12):2573-2586.
1062 31. Steele JA, Countway PD, Xia L, Vigil PD, Beman JM, Kim DY, Chow CE,
1063 Sachdeva R, Jones AC, Schwalbach MS *et al*. Marine bacterial, archaeal and
1064 protistan association networks reveal ecological linkages. ISME J. 2011;
1065 5(9):1414-1425.
1066 32. Needham DM, Fuhrman JA. Pronounced daily succession of phytoplankton,
1067 archaea and bacteria following a spring bloom. Nat Microbiol. 2016;
1068 1(4):16005.
1069 33. Deutschmann IM, Lima-Mendez G, Krabberød AK, Raes J, Vallina SM, Faust
1070 K, Logares R. Disentangling environmental effects in microbial association
1071 networks. preprint. 2021.
1072 34. Giner CR, Balague V, Krabberod AK, Ferrera I, Rene A, Garces E, Gasol JM,
1073 Logares R, Massana R. Quantifying long-term recurrence in planktonic
1074 microbial eukaryotes. Mol Ecol. 2019; 28(5):923-935.
1075 35. Alonso-Saez L, Balague V, Sa EL, Sanchez O, Gonzalez JM, Pinhassi J,
1076 Massana R, Pernthaler J, Pedros-Alio C, Gasol JM. Seasonality in bacterial
1077 diversity in north-west Mediterranean coastal waters: assessment through clone
1078 libraries, fingerprinting and FISH. FEMS Microbiol Ecol. 2007; 60(1):98-112.
1079 36. Gasol JM, Cardelus C, Moran XAG, Balague V, Forn I, Marrase C, Massana
1080 R, Pedros-Alio C, Sala MM, Simo R *et al*. Seasonal patterns in phytoplankton
1081 photosynthetic parameters and primary production at a coastal NW
1082 Mediterranean site. Sci Mar. 2016; 80(S1):63-77.

37. Watts DJ, Strogatz SH. Collective dynamics of 'small-world' networks. Nature. 1998; 393(6684):440-442.
38. Pedrós-Alió C. The rare bacterial biosphere. Ann Rev Mar Sci. 2012; 4:449-466.
39. Mestre M, Höfer J, Sala MM, Gasol JM. Seasonal Variation of Bacterial Diversity Along the Marine Particulate Matter Continuum. Front Microbiol. 2020; 11(1590).
40. Auladell A, Sánchez P, Sánchez O, Gasol JM, Ferrera I. Long-term seasonal and interannual variability of marine aerobic anoxygenic photoheterotrophic bacteria. ISME J. 2019; 13(8):1975-1987.
41. Berdjeb L, Parada A, Needham DM, Fuhrman JA. Short-term dynamics and interactions of marine protist communities during the spring-summer transition. ISME J. 2018; 12:1907–1917.
42. Lambert S, Tragin M, Lozano JC, Ghiglione JF, Vaulot D, Bouget FY, Galand PE. Rhythmicity of coastal marine picoeukaryotes, bacteria and archaea despite irregular environmental perturbations. ISME J. 2019; 13(2):388-401.
43. Charles F, Lantoine F, Brugel S, Chrétiennot-Dinet M-J, Quiroga I, Rivière B. Seasonal survey of the phytoplankton biomass, composition and production in a littoral NW Mediterranean site, with special emphasis on the picoplanktonic contribution. Estuarine, Coastal and Shelf Science. 2005; 65(1):199-212.
44. Milici M, Deng Z-L, Tomasch J, Decelle J, Wos-Oxley ML, Wang H, Jáuregui R, Plumeier I, Giebel H-A, Badewien TH *et al*. Co-occurrence Analysis of Microbial Taxa in the Atlantic Ocean Reveals High Connectivity in the Free-Living Bacterioplankton. Front Microbiol. 2016; 7(649).
45. Newman M. Networks: Oxford University Press; 2018.
46. Coyte KZ, Schluter J, Foster KR. The ecology of the microbiome: Networks, competition, and stability. Science. 2015; 350:663-666.
47. Vellend M. The theory of ecological communities. Princeton: Princeton University Press; 2016.
48. Stouffer DB, Bascompte J. Compartmentalization increases food-web persistence. Proceedings of the National Academy of Sciences. 2011; 108:3648-3652.
49. Krause AE, Frank KA, Mason DM, Ulanowicz RE, Taylor WW. Compartments revealed in food-web structure. Nature. 2003; 426(6964):282-285.
50. Olesen JM, Bascompte J, Dupont YL, Jordano P. The modularity of pollination networks. Proceedings of the National Academy of Sciences. 2007; 104:19891-19896.
51. Medeiros LP, Garcia G, Thompson JN, Guimarães PR. The geographic mosaic of coevolution in mutualistic networks. Proceedings of the National Academy of Sciences. 2018; 115:12017-12022.
52. Tripp HJ, Schwalbach MS, Meyer MM, Kitner JB, Breaker RR, Giovannoni SJ. Unique glycine-activated riboswitch linked to glycine–serine auxotrophy in SAR11. Environ Microbiol. 2009; 11(1):230-238.
53. Carini P, Steindler L, Beszteri S, Giovannoni SJ. Nutrient requirements for growth of the extreme oligotroph '*Candidatus Pelagibacter* ubique' HTCC1062 on a defined medium. ISME J. 2013; 7(3):592-602.
54. Carini P, Campbell EO, Morré J, Sañudo-Wilhelmy SA, Cameron Thrash J, Bennett SE, Temperton B, Begley T, Giovannoni SJ. Discovery of a SAR11 growth requirement for thiamin's pyrimidine precursor and its distribution in the Sargasso Sea. ISME J. 2014; 8(8):1727-1738.

55. Włodarczyk A, Selão TT, Norling B, Nixon PJ. Newly discovered *Synechococcus* sp. PCC 11901 is a robust cyanobacterial strain for high biomass production. Communications Biology. 2020; 3(1):215.
56. Becker JW, Hogle SL, Rosendo K, Chisholm SW. Co-culture and biogeography of *Prochlorococcus* and SAR11. ISME J. 2019; 13(6):1506-1519.
57. Chafee M, Fernàndez-Guerra A, Buttigieg PL, Gerdts G, Eren AM, Teeling H, Amann RI. Recurrent patterns of microdiversity in a temperate coastal marine environment. ISME J. 2018; 12(1):237-252.
58. Paine RT. A Note on Trophic Complexity and Community Stability. The American Naturalist. 1969; 103(929):91-93.
59. Banerjee S, Schlaeppi K, van der Heijden MGA. Keystone taxa as drivers of microbiome structure and functioning. Nat Rev Microbiol. 2018; 16:567-576.
60. Berry D, Widder S. Deciphering microbial interactions and detecting keystone species with co-occurrence networks. Front Microbiol. 2014; 5(MAY):219.
61. Freilich MA, Wieters E, Broitman BR, Marquet PA, Navarrete SA. Species co-occurrence networks: Can they reveal trophic and non-trophic interactions in ecological communities? Ecology. 2018; 99(3):690-699.
62. Banerjee S, Kirkby CA, Schmutter D, Bissett A, Kirkegaard JA, Richardson AE. Network analysis reveals functional redundancy and keystone taxa amongst bacterial and fungal communities during organic matter decomposition in an arable soil. Soil Biology and Biochemistry. 2016; 97:188-198.
63. Pester M, Bittner N, Deevong P, Wagner M, Loy A. A 'rare biosphere' microorganism contributes to sulfate reduction in a peatland. ISME J. 2010; 4(12):1591-1602.
64. Zhu F, Massana R, Not F, Marie D, Vaulot D. Mapping of picoeucaryotes in marine ecosystems with quantitative PCR of the 18S rRNA gene. FEMS Microbiol Ecol. 2005; 52(1):79-92.
65. Seymour JR, Amin SA, Raina JB, Stocker R. Zooming in on the phycosphere: the ecological interface for phytoplankton-bacteria relationships. Nat Microbiol. 2017; 2:17065.
66. Farnelid HM, Turk-Kubo KA, Zehr JP. Identification of Associations between Bacterioplankton and Photosynthetic Picoeukaryotes in Coastal Waters. Front Microbiol. 2016; 7(339).
67. Auladell A, Barberán A, Logares R, Garcés E, Gasol JM, Ferrera I. Seasonal niche differentiation between evolutionary closely related marine bacteria. bioRxiv. 2020.
68. Grasshoff K, Kremling K, Ehrhardt M. Methods of Seawater Analysis: Third, Completely Revised and Extended Edition; 2007.
69. Massana R, Castresana J, Balague V, Guillou L, Romari K, Groisillier A, Valentin K, Pedros-Alio C. Phylogenetic and ecological analysis of novel marine stramenopiles. Appl Environ Microbiol. 2004; 70(6):3528-3534.
70. Stoeck T, Bass D, Nebel M, Christen R, Jones MD, Breiner HW, Richards TA. Multiple marker parallel tag environmental DNA sequencing reveals a highly complex eukaryotic community in marine anoxic water. Mol Ecol. 2010; 19 Suppl 1(SUPPL. 1):21-31.
71. Herlemann DPR, Labrenz M, Jürgens K, Bertilsson S, Waniek JJ, Andersson AF. Transitions in bacterial communities along the 2000 km salinity gradient of the Baltic Sea. ISME J. 2011; 5(10):1571-1579.

1181 72. Apprill A, McNally S, Parsons R, Weber L. Minor revision to V4 region SSU
1182 rRNA 806R gene primer greatly increases detection of SAR11
1183 bacterioplankton. Aquat Microb Ecol. 2015; 75(2):129-137.
1184 73. Martin M. Cutadapt removes adapter sequences from high-throughput
1185 sequencing reads. EMBnet Journal. 2011; 17(1):10-12.
1186 74. Callahan BJ, McMurdie PJ, Rosen MJ, Han AW, Johnson AJ, Holmes SP.
1187 DADA2: High-resolution sample inference from Illumina amplicon data. Nat
1188 Methods. 2016; 13(7):581-583.
1189 75. Wang Q, Garrity GM, Tiedje JM, Cole JR. Naive Bayesian classifier for rapid
1190 assignment of rRNA sequences into the new bacterial taxonomy. Appl Environ
1191 Microbiol. 2007; 73(16):5261-5267.
1192 76. Quast C, Pruesse E, Yilmaz P, Gerken J, Schweer T, Yarza P, Peplies J,
1193 Glockner FO. The SILVA ribosomal RNA gene database project: improved
1194 data processing and web-based tools. Nucleic Acids Res. 2013; 41(Database
1195 issue):D590-596.
1196 77. Altschul SF, Gish W, Miller W, Myers EW, Lipman DJ. Basic local alignment
1197 search tool. Journal of molecular biology. 1990; 215(3):403-410.
1198 78. Guillou L, Bachar D, Audic S, Bass D, Berney C, Bittner L, Boutte C, Burgaud
1199 G, de Vargas C, Decelle J *et al*. The Protist Ribosomal Reference database
1200 (PR2): a catalog of unicellular eukaryote small sub-unit rRNA sequences with
1201 curated taxonomy. Nucleic Acids Res. 2013; 41(Database issue):D597-604.
1202 79. McNichol J, Berube PM, Biller SJ, Fuhrman JA. Evaluating and Improving
1203 SSU rRNA PCR Primer Coverage via Metagenomes from Global Ocean
1204 Surveys. bioRxiv. 2020.
1205 80. Oksanen J, Guillaume Blanchet FFM, Kindt R, Legendre P, McGlinn D,
1206 Minchin PR, O'Hara RB, Simpson GL, Solymos P, Stevens MHH *et al*. vegan:
1207 Community Ecology Package. R package. In.; 2016.
1208 81. Moritz S. imputeTS: Time Series Missing Value Imputation. In.; 2017.
1209 82. Dufrêne M, Legendre P. Species assemblages and indicator species: The need
1210 for a flexible asymmetrical approach. Ecological Monographs. 1997.
1211 83. Roberts DW. labdsv: Ordination and Multivariate Analysis for Ecology. R
1212 package version 1.8-0. In.; 2016.
1213 84. Ruan Q, Dutta D, Schwalbach MS, Steele JA, Fuhrman JA, Sun F. Local
1214 similarity analysis reveals unique associations among marine bacterioplankton
1215 species and environmental factors. Bioinformatics. 2006; 22(20):2532-2538.
1216 85. Xia LC, Ai D, Cram JA, Liang X, Fuhrman JA, Sun F. Statistical significance
1217 approximation in local trend analysis of high-throughput time-series data using
1218 the theory of Markov chains. BMC Bioinformatics. 2015; 16(1):301.
1219 86. Xia LC, Ai D, Cram J, Fuhrman JA, Sun F. Efficient statistical significance
1220 approximation for local similarity analysis of high-throughput time series data.
1221 Bioinformatics. 2013; 29(2):230-237.
1222 87. Deutschmann IM, Lima-Mendez G, Krabberød AK, Raes J, Vallina SM, Faust
1223 K, Logares R. Disentangling environmental effects in microbial association
1224 networks. ResearchSquare. 2020.
1225 88. Erdős P, Rényi A. On random graphs. Publicationes Mathematicae. 1959;
1226 6:290–297.
1227 89. Banerjee S, Baah-Acheamfour M, Carlyle CN, Bissett A, Richardson AE,
1228 Siddique T, Bork EW, Chang SX. Determinants of bacterial communities in
1229 Canadian agroforestry systems. Environ Microbiol. 2016; 18(6):1805-1816.

90. Yu G, Chen Y-s, Guo Y-c. Design of integrated system for heterogeneous network query terminal. Journal of Computer Applications. 2009; 29(8):2191-2193.
91. Bastian M, Heymann S, Jacomy M. Gephi: an open source software for exploring and manipulating networks. In: *International AAAI Conference on Weblogs and Social Media*. 2009.
92. Smoot ME, Ono K, Ruscheinski J, Wang PL, Ideker T. Cytoscape 2.8: New features for data integration and network visualization. Bioinformatics. 2011.
93. Bader GD, Hogue CW. An automated method for finding molecular complexes in large protein interaction networks. BMC Bioinformatics. 2003; 4(1):2.

1242 **Supplementary Figures**
1243

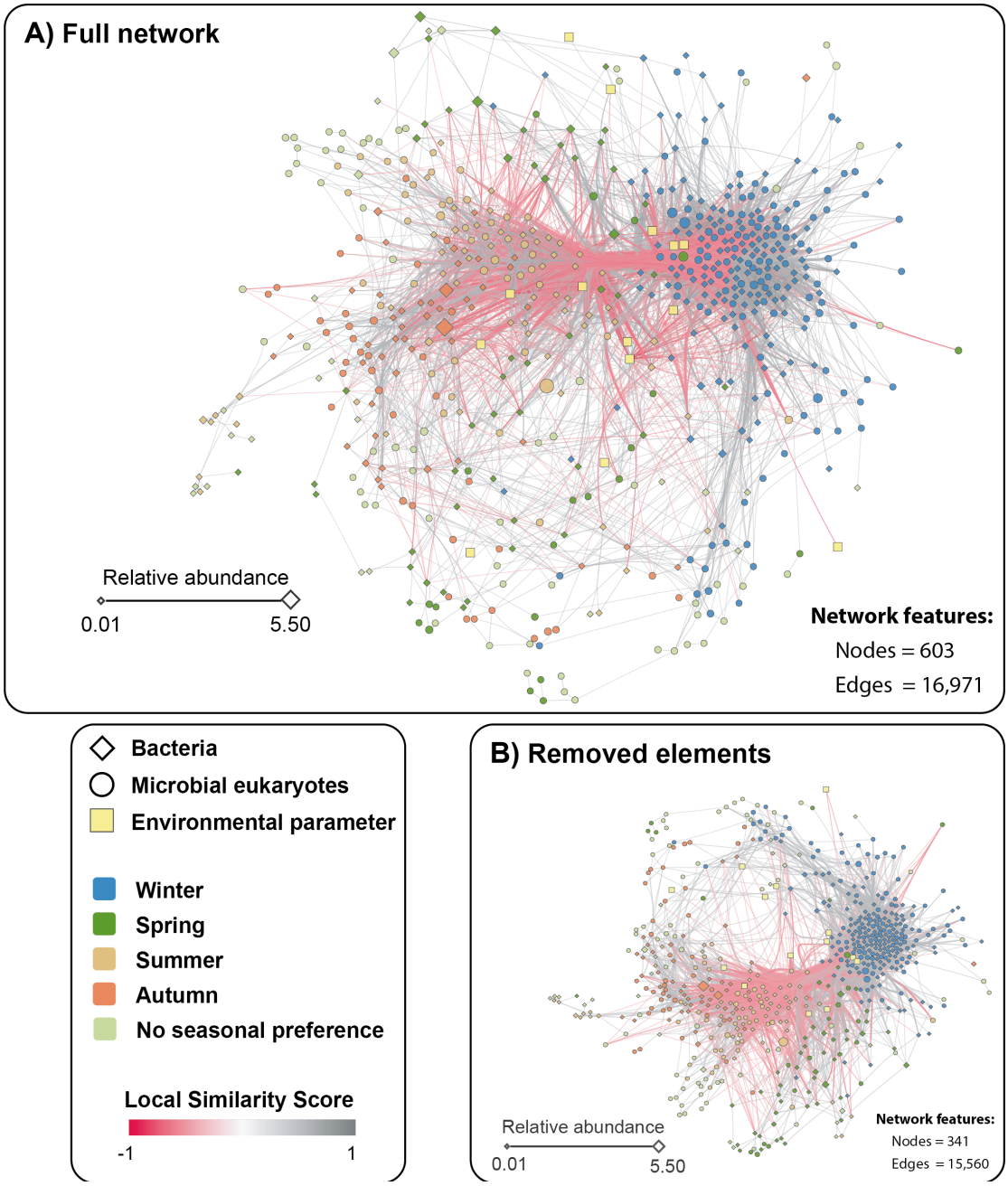

1244
1245
1246 **Supplementary Figure 1. Panel A** shows the full network constructed with the
1247 resident microbiota (that is, OTUs present in >30% of the samples over 10 years; Table
1248 1). **Panel B** displays network elements that were removed as they did not fulfill the cut-
1249 offs (that is, highly significant correlations (P & Q <0.001), local similarity scores >|0.7|
1250 and Spearman correlations >|0.7|).
1251
1252

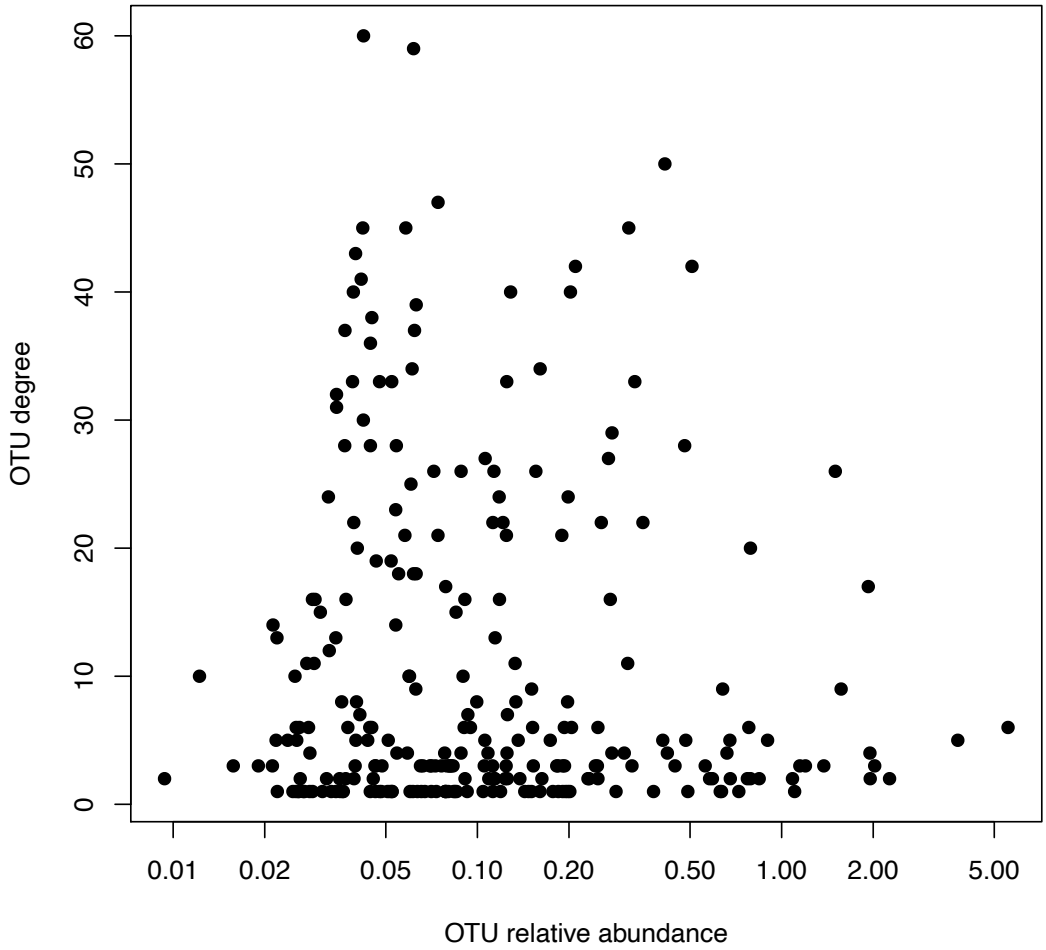

Supplementary Figure 2. OTU relative abundance vs. degree shows no relationship in the core network.